American Mineralogist, Volume 80, pages 115–130, 1995

Ca-rich carbonate melts: A regular-solution model, with applications to carbonatite magma + vapor equilibria and carbonate lavas on Venus

ALLAN H. TREIMAN
Lunar and Planetary Institute, 3600 Bay Area Boulevard, Houston, Texas 77058-1113, U.S.A.

ABSTRACT

A thermochemical model of the activities of species in carbonate-rich melts would be useful in quantifying chemical equilibria between carbonatite magmas and vapors and in extrapolating liquidus equilibria to unexplored *PTX*. A regular-solution model of Ca-rich carbonate melts is developed here, using the fact that they are ionic liquids, and can be treated (to a first approximation) as interpenetrating regular solutions of cations and of anions. Thermochemical data on systems of alkali metal cations with carbonate and other anions are drawn from the literature; data on systems with alkaline earth (and other) cations and carbonate (and other) anions are derived here from liquidus phase equilibria. The model is validated in that all available data (at 1 kbar) are consistent with single values for the melting temperature and heat of fusion for calcite, and all liquidi are consistent with the liquids acting as regular solutions.

At 1 kbar, the metastable congruent melting temperature of calcite ($CaCO_3$) is inferred to be 1596 K, with $\Delta\overline{H}_{fus}$(calcite) = 31.5 ± 1 kJ/mol. Regular solution interaction parameters (W) for Ca^{2+} and alkali metal cations are in the range −3 to −12 kJ/mol²; W for Ca^{2+}-Ba^{2+} is approximately −11 kJ/mol²; W for Ca^{2+}-Mg^{2+} is approximately −40 kJ/mol², and W for Ca^{2+}-La^{3+} is approximately +85 kJ/mol². Solutions of carbonate and most anions (including OH^-, F^-, and SO_4^{2-}) are nearly ideal, with W between 0 (ideal) and −2.5 kJ/mol². The interaction of carbonate and phosphate ions is strongly nonideal, which is consistent with the suggestion of carbonate-phosphate liquid immiscibility. Interaction of carbonate and sulfide ions is also nonideal and suggestive of carbonate-sulfide liquid immiscibility. Solution of H_2O, for all but the most H_2O-rich compositions, can be modeled as a disproportionation to hydronium (H_3O^+) and hydroxyl (OH^-) ions with W for Ca^{2+}-H_3O^+ ≈ 33 kJ/mol².

The regular-solution model of carbonate melts can be applied to problems of carbonatite magma + vapor equilibria and of extrapolating liquidus equilibria to unstudied systems. Calculations on one carbonatite (the Husereau dike, Oka complex, Quebec, Canada) show that the anion solution of its magma contained an OH^- mole fraction of ~0.07, although the vapor in equilibrium with the magma had $P(H_2O) = 8.5 \times P(CO_2)$. F in carbonatite systems is calculated to be strongly partitioned into the magma (as F^-) relative to coexisting vapor. In the Husereau carbonatite magma, the anion solution contained an F^- mole fraction of $\sim 6 \times 10^{-5}$.

Calcite and anhydrite may be present on the surface of Venus, but they would not be molten at ambient surface temperature (660–760 K) because the minimum melt temperature (eutectic) for the calcite + anhydrite system is calculated to be 1250 K. The Venus atmosphere contains 5 ppb HF, which implies that the anion solution of a carbonate-rich magma in equilibrium with the atmosphere would contain a F^- mole fraction of $\sim 7 \times 10^{-3}$, or about 0.1 wt%. Although this proportion of F is much enriched compared with the atmosphere, it would have little effect on phase relations of the carbonatite.

INTRODUCTION

Carbonatites are igneous rocks that formed from carbonate-rich magmas. The petrogeneses of carbonatites are imperfectly understood, in part because of uncertainties in the physical and chemical properties of their parent magmas. Although the physical and mass-transport properties of carbonatite magmas are becoming appreciated (Treiman and Schedl, 1983; Dawson et al., 1990; Keller and Krafft, 1990; Watson, 1991; Norton and Pinkerton, 1992), their thermochemical properties have been studied little (Bradley, 1962; Treiman, 1989). Thus, investigations of carbonatites have not benefited from quantitative thermochemical models such as have been developed for silicate magmas (e.g., Ghiorso et al., 1983; Berman and Brown, 1987; Ghiorso, 1987).

0003–004X/95/0102–0115$02.00

For instance, a thermochemical model of carbonate melts would provide a quantitative link between the compositions of carbonatite magmas and the compositions of their associated volatile phases. Carbon dioxide is obviously important in carbonatite magmas; H_2O has played a prominent role in experimental studies of carbonatite genesis (Wyllie, 1989), and the potential importance of F has recently been reemphasized (Gittins et al., 1990; Jago and Gittins, 1991). In addition, most plutonic carbonatites are surrounded by volumetrically significant zones of metasomatized rock, i.e., fenite (McKie, 1966). These zones bespeak large fluxes of volatiles associated with carbonatite magmas. It has been possible to constrain the composition of the volatile phases through the compositions and phases of the solids with which they equilibrated (e.g., Rubie and Gunter, 1983; Treiman and Essene, 1984; Kresten and Morogan, 1986; Andersen, 1986). However, it has been impossible to constrain compositions of carbonatite magma from fluid compositions, except in the most general terms. With a quantitative thermochemical model of carbonatite magmas, the connection between fluid and magma compositions would be straightforward.

Similarly, a thermochemical model of carbonate melts would permit extrapolation of known liquidus equilibria to physical and chemical conditions that have not been studied experimentally. In this way, a thermochemical model would provide a structure for understanding the results of experiments already completed, a ready way of applying experimental results to complex natural systems, and an aid in designing new experimental programs.

In this paper, I propose a thermochemical model of carbonate-rich magmas, based on regular-solution theory and the observation that carbonatite magmas are ionic liquids (Treiman and Schedl, 1983). In the model, all available data (at 1 kbar) are consistent with a single temperature of melting for calcite (metastable congruent melting), and a single value for the heat of fusion for calcite. Similarly, the locations of all liquidus calcite-saturated liquidus surfaces are consistent with the Ca-rich carbonate melts being regular solutions. Portions of this model were presented by Treiman (1989), which is superseded by this work.

Temkin melt model

Carbonate-rich melts are ionic melts or fused salts, liquids in which the discrete entities (ions) are charged and bound by electrostatic forces (Zarzycki, 1962; Sundheim, 1964; Lumsden, 1966; Kleppa, 1977, 1981). Polymerization of anions (as in silicate liquids) is unimportant, and ionic complexes can be treated as distinct ionic species.

Ionic liquids are amenable to relatively simple thermochemical analysis because their cations and anions may be treated, to a first approximation, as independent solutions. This approximation is the quasi-lattice or Temkin (1945) model. It is justifiable because enormous energy would be needed to exchange, for instance, a cation surrounded by anions for an anion surrounded by anions (Blander, 1964). The Temkin model is consistent with ideal behavior in each ion solution and also with regular behavior, in which there is heat of mixing but no excess entropy of mixing (Førland, 1955). Here, I use the simplest version of the Temkin model, in which all cations occupy identical quasi-lattice sites, as do all anions. This model ignores complexation except as reflected by regular solution behavior and ignores the expectation of differing sites in the liquid quasi-lattice. The Temkin model is only an approximation because local charge balance does not permit ions of different charges to interchange completely freely (e.g., Ca^{2+} vs. Na^{+}) and because common sense (and the Gibbs-Duhem relation) suggest that different ions affect their surrounding ions in different ways. For instance, one cannot expect ions of different sizes (e.g., Ca^{2+} vs. Mg^{2+}) and charges (e.g., Ca^{2+} vs. Na^{+}) to maintain identical distances and coordinations with surrounding ions.

With these caveats, the Temkin model is a good first approximation for the properties of many ionic liquids, including (as I show below) those of Ca- and carbonate-rich melts to the level of detail permitted by most available data. In addition, the regular solution model is familiar in the geological community and is the simplest formulation of real solutions (e.g., Ghiorso et al., 1983; Ghiorso, 1987; Berman and Brown, 1987; Helffrich and Wood, 1989). More physically accurate models for ionic salts (e.g., the reciprocal-salt or conformal-solution model: Blander and Topol, 1966; Kleppa, 1977, 1981) may be better representations of reality, but they are not justified by the quality and quantity of data available.

Interpretative method

For some components in carbonate magmas, thermochemical data can be taken directly from the literature. But for many major components, like Ca and Mg carbonates, and for magmas at high pressure, such data must be gained indirectly. The most accessible sources of these data are liquidus phase equilibria (in effect, measurements of freezing point depressions), which can be manipulated to retrieve heats of fusion and activity-composition relationships (Lewis and Randall, 1961).

To simplify the interpretation of liquidus surfaces, solid and liquid phases both must be referred to the same standard state. For simplicity and consistency with geological applications, the standard state for a component is taken as the chemically pure phase in its equilibrium structure at the temperature of interest. Thus, pure solid phases below their melting temperatures have activities of unity; hypothetical pure liquids below their solidification temperatures have activities exceeding unity. Activities of components in solutions (solid and liquid) are referred to the same standard state. For solid phases below their melting temperatures, this is a normal solvent standard state: the ratio of activity to mole fraction for a component (a/X) is unity for the pure component ($X = 1$). For liquid solutions phases, this is also a solvent solid state, but with the pure solvent having nonunit activity at subsolidification temperatures. The hypothetical pure liquid in its standard state must have the same structure

as the solution, which need not be the same liquid structure as in the pure system at its melting temperature.

Freezing point depression is treated in detail in standard thermodynamics textbooks (e.g., Lewis and Randall, 1961). Consider the isobaric melting reaction A (solid) $\rightleftharpoons$ A (liquid solution) in the system A-B at $T < T_{fus}$, the congruent melting temperature of A (solid). One can approach this state in two steps: melting of pure A at $T < T_{fus}$, and isothermal solution of B into the melt and solid until they are at equilibrium. For the first step, the free energy of melting pure A at a temperature below $T < T_{fus}$ is given as

$$\Delta\overline{G}^{T}_{fus} = \Delta\overline{H}^{0}_{fus}\left(1 - \frac{T}{T_{fus}}\right) \quad (1)$$

where $\Delta\overline{H}^{0}_{fus}(A)$ is the molar enthalpy change on melting (heat of fusion) of pure phase A at T_{fus} (viz., Flood et al., 1949; Lewis and Randall, 1961, p. 415). Equation 1 assumes that the heat of fusion is not a function of temperature, i.e., the effect of $\Delta\overline{C}_{P,fus}(A)$ on melting A is relatively small, which is justifiable for carbonate melt systems at the present level of precision. Ignoring $\Delta\overline{C}_{P,fus}$ in carbonate, chloride, or nitrate systems causes <1% error in the $\Delta\overline{H}_{fus}$ and <10% error in regular solution parameters (Treiman, unpublished calculations). This $\Delta\overline{G}^{T}_{fus}(A)$ is positive because a melt of pure A composition is not stable relative to the solid at $T < T_{fus}$. The second step is isothermal solution of B into the melt and solid until they are at equilibrium, i.e., $\Delta\overline{G}^{T}_{fus}(A) + \Delta\overline{G}^{T}_{solution} = 0$. Substituting this and the definition of free energy changes with composition into Equation 1 yields a description of the liquidus surface,

$$\left(1 - \frac{T}{T_{fus}}\right)\Delta\overline{H}^{0}_{fus}(A) = -RT(\ln a_{A,melt} - \ln a_{A,solid}) \quad (2)$$

where a is activity of a component in a phase, relative to the standard states given above.

The activity of A in the melt phase can be calculated from the assumption of regular solution behavior by means of the activity coefficient γ_A

$$\gamma_A = a_A/X_A. \quad (3)$$

For a multicomponent solution of species A, B, and C, the heat of mixing is given as

$$\Delta H_{mix} = (n_A + n_B + n_C)(X_A X_B W_{AB} + X_A X_C W_{AC} + X_B X_C W_{BC} + X_A X_B X_C W_{ABC}) \quad (4)$$

where n is the number of moles of a species present, and W is the interaction parameter for that pair (or triplet) of species (Lewis and Randall, 1961). The ternary interaction parameter is assumed here to be zero, although this value is not required by theory (Helffrich and Wood, 1989). The activity coefficient γ for species A is then

$$RT \ln \gamma_A = (X_B^2 + X_B X_C)W_{AB} + (X_C^2 + X_B X_C)W_{AC} - X_B X_C W_{BC} \quad (5)$$

(Andersen and Lindsley, 1981). In an ideal solution, all $W = 0$, and so $\gamma = 1$. In the Temkin model of ionic liquids, the cations and anions are treated independently as regular solutions, each with its own X, n, W, and γ terms. Substituting Equations 3 and 5 into Equation 2 for the system A-B and rearranging into the format $y = ax + b$ yields

$$-\frac{RT \ln(X_{A,melt}) - RT \ln(a_{A,solid})}{1 - \frac{T}{T_{fus}}} = W_{AB}\frac{(1 - X_{A,melt})^2}{1 - \frac{T}{T_{fus}}} + \Delta\overline{H}^{0}_{fus}(A). \quad (6)$$

If the phase A is purely component A, its activity is unity, and Equation 6 simplifies to

$$-\frac{RT \ln(X_{A,melt})}{1 - \frac{T}{T_{fus}}} = W_{AB}\frac{(1 - X_{A,melt})^2}{1 - \frac{T}{T_{fus}}} + \Delta\overline{H}^{0}_{fus}(A). \quad (7)$$

For points on this A-saturated liquidus, a graph of $-RT \ln(X_{A,melt})/(1 - T/T_{fus})$ vs. $(1 - X_{A,melt})^2/(1 - T/T_{fus})$ should yield a straight line of slope W_{AB} and intercept $\Delta\overline{H}^{0}_{fus}(A)$ (e.g., Flood et al., 1949). Typically, phase-equilibrium experiments yield bracketed ranges in T and X within which a liquidus must lie, and so this graph would consist of brackets through which the straight line must pass. These brackets can typically be satisfied by ranges of W_{AB} and $\Delta\overline{H}^{0}_{fus}(A)$.

These descriptions of the liquidus surface can be related to the Temkin model of ionic melts with a few definitions of standard state for ion activities. As with solid and liquid phases, the reference state for an ionic species is a crystalline solid containing that pure ionic species at the temperature of interest. For example, systems in equilibrium with the pure solid phase $L^{n+}M^{n-}$ have activities of ionic components L^{n+} and M^{n-} of unity. If a solution phase contains both L^{n+} and M^{n-} ions,

$$a_{L^{n+}M^{n-}} = a_{L^{n+}} \cdot a_{M^{n-}}. \quad (8)$$

If a solid phase contains only a single cation or anion species, the activity of that ion species is unity, and the activity of the phase is equal to the activity of the other ion species. Activities of individual ion species in melt solutions can be determined by their mole fractions and regular solution interaction parameters (Eqs. 3 and 5). The activity of a component in a melt solution is referenced, as before, to the pure component in its equilibrium phase at that T. Thus, in a melt in equilibrium with solid, pure $L^{n+}M^{n-}$, the activity product $a_{L^{n+}} \cdot a_{M^{n-}}$ is unity.

Other thermochemical quantities are calculated with standard methods. The molar entropy of melting is calculated from the heat of melting as

$$\Delta\overline{S}_{fus} = \Delta\overline{H}_{fus}/T_{fus} \quad (9)$$

TABLE 1. Melting of alkali and alkaline earth carbonates: Molar properties at 1 bar

Compound	T_{fus} K	$\Delta\overline{H}^{0}_{fus}$ kJ/mol	$\Delta\overline{S}^{0}_{fus}$ J/(mol·K)	$\Delta\overline{C}_{P,fus}$ J/(mol·K)	$\Delta\overline{V}_{fus}$ cm³/mol
Na_2CO_3	1131	29.7	26.3	−8.5	4.7*
K_2CO_3	1171	27.6	23.6	−1.1	7.5**
Li_2CO_3	996	44.8	44.8	−7.6	2.6
$CaCO_3$†	1583	30.5 ± 1	19 ± 2.5	—	—
$CaCO_3$‡	1463	38.5 ± 4	26 ± 3	—	—

Note: enthalpy and entropy from Janz et al. (1979), heat capacities from Selman and Maru (1981), and volumes from Klement and Cohen (1975) and Janz et al. (1979).

* Volume from Klement and Cohen (1975). Janz et al. (1979) gave 7.5 cm³/mol.

** Volume from Klement and Cohen (1975). Janz et al. (1979) gave 10.3 cm³/mol.

† Appropriate for Ca-rich melts, and those containing significant K vs. Na. Recalculated from Førland (1955), using T_{fus} extrapolated from high pressure. These data are consistent with high-pressure determinations; see text.

‡ Appropriate for lower temperature, Na-rich melts. Recalculated from Førland (1955) and Flood et al. (1949).

TABLE 2. Melting of alkali and alkaline earth carbonates: Molar properties at 1 kbar

Compound	T_{fus} K	$\Delta\overline{H}^{0}_{fus}$ kJ/mol	$\Delta\overline{S}^{0}_{fus}$ J/(mol·K)	$\Delta\overline{C}_{P,fus}$ J/(mol·K)	$\Delta\overline{V}_{fus}$ cm³/mol
Na_2CO_3	1145*	30.1	26.3	−8.0	4.7
K_2CO_3	1200*	28.2	23.5	−1.1	4.8
Li_2CO_3	1003**	45.0	45.0	−7.6	2.6
$CaCO_3$	1596†	31.5 ± 1	19.7 ± 0.7	—	2.5 ± 0.1
$MgCO_3$‡	1750	32 ± 25?	18 ± 15?	—	0.7 ± 0.6?

Note: heats and entropies of alkali carbonates extrapolated from 1-bar values; T_{fus} measured; volumes from high-pressure phase equilibria. Data for alkaline earth carbonates as derived in text.

* Koster van Groos and Wyllie (1966).

** Klement and Cohen (1975).

† Extrapolated from Irving and Wyllie (1975); see text.

‡ T_{fus} extrapolated from Irving and Wyllie (1975). Other values estimated from liquidus surface of Ragone et al. (1966) without consideration of possible experimental errors. See text.

because congruent melting of a pure phase is isothermal. Volume changes on melting can be derived from direct measurement or from polybaric equilibria by the Clausius-Clapeyron equation:

$$\Delta\overline{V}_{fus} = \frac{\Delta\overline{S}_{fus}}{(dP/dT)_{fus}}. \quad (10)$$

Extrapolation of heats of melting over temperatures and pressures follow from the partial derivatives of enthalpy:

$$\frac{\partial\Delta\overline{H}_{fus}}{\partial T} = \Delta\overline{C}_{P,fus} \quad \text{and} \quad \frac{\partial\Delta\overline{H}_{fus}}{\partial P} = \Delta\overline{V}_{fus} \quad (11)$$

where $\Delta\overline{C}_{P,fus}$ is the difference in heat capacities between molten and solid phases (Tables 1 and 2). Note that $\Delta\overline{C}_{P,fus}$ is negative for the alkali carbonates (Tables 1 and 2), as it is for many ionic salts (Robie et al., 1979; DeKock, 1986). A negative $\Delta\overline{C}_{P,fus}$ suggests premelting structural changes in the solid and does not violate the second law of thermodynamics.

ALKALI CARBONATES

Alkali carbonates are inferred to be important constituents of some carbonate magmas (LeBas, 1981; Dawson et al., 1987; Gittins, 1989), although few carbonatites contain alkali carbonate minerals. There is an extensive literature on melting and mixing properties of the alkali carbonates, from which much of Table 1 is drawn directly or calculated.

For volume changes on fusion, $\Delta\overline{V}_{fus}$, for the alkali carbonates (Table 1), the data of Klement and Cohen (1975) are preferred over those of Janz et al. (1979), which are larger than those of Klement and Cohen by ~20%. The discrepancy in $\Delta\overline{V}_{fus}$ lies in the volumes of the solid phases, as both groups report comparable melt volumes. Klement and Cohen's (1975) data are preferred, because their solid volumes are from high-temperature X-ray diffraction, rather than from density measurement (used by Janz et al., 1979).

CALCIUM CARBONATE

Calcite is the most abundant mineral in most carbonatites, intrusive and extrusive (Bailey, 1993), and so calcium carbonate is likely to be among the most important components in carbonate magmas. The melting properties of $CaCO_3$ at 1 bar and 1 kbar must be inferred indirectly because calcite does not melt congruently at these pressures; pure calcite decarbonates below 40 bars (Baker, 1962) and melts incongruently to liquid + vapor between 90 and ~7000 bars (Irving and Wyllie, 1975; Huang and Wyllie, 1976). However, melting and solution properties of $CaCO_3$ can be measured directly for melts that are not too rich in $CaCO_3$ component, given a temperature for its (metastable) congruent melting.

All high-pressure liquidus surfaces and most 1-bar liquidus surfaces are consistent with a single value for the temperature of melting (T_{fus}) and heat of fusion $\Delta\overline{H}^{0}_{fus}$(calcite); unless specifically noted, all discussion here refers to numerical values consistent with 1-kbar liquidus equilibria. However, some 1-bar liquidi are consistent with a separate set of T_{fus} and $\Delta\overline{H}^{0}_{fus}$(calcite) (Table 1); it is possible that Ca-rich carbonate melt might occur in two distinct structures at 1 bar (viz., Førland, 1955). For the most part, melting properties derived for high pressure are appropriate for geological applications.

Melting temperature

The congruent melting temperature for pure $CaCO_3$ in the calcite structure, T_{fus}(calcite), can be estimated by extrapolating the high-pressure congruent melting curve to lower pressures (Irving and Wyllie, 1975; Huang and Wyllie, 1976). Between 10 and 20 kbar, the congruent melting curve for $CaCO_3$ has a slope of −12.5 K/kbar, implying a congruent T_{fus}(calcite) of 1583 K at 1 bar and 1596 K at 1 kbar (Tables 1 and 2). This 1-kbar T_{fus}(calcite) is just above the experimentally determined bracket for

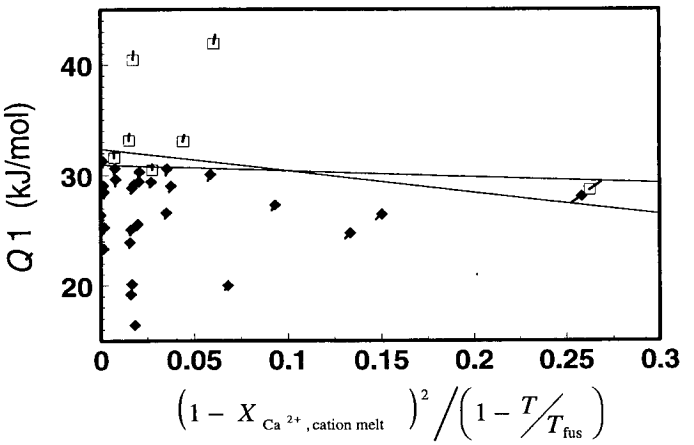

Fig. 1. Regular-solution interpretation of calcite-saturated liquidus in $CaCO_3$-$BaSO_4$-CaF_2 (500 bars CO_2, Kuellmer et al., 1966), following Eq. 12. See Table 3 for definition of $Q1$. Open and filled symbols represent liquid-only and liquid + calcite experiments, respectively. Lines from each data point represent a conservative estimate of errors (±5 K in T; ±0.2 wt% in X), showing only the error bar halves that contribute to uncertainty in slope and intercept. The liquidus surfaces, linear with slope W and ordinate intercept of $\Delta\overline{H}^0_{fus}$(calcite), should lie between these groups of experiments. Within error, all data are consistent with $\Delta\overline{H}^0_{fus}$(calcite) = 31.5 ± 1 kJ/mol and $W_{Ca^{2+}\text{-}Ba^{2+}} = -11 \pm 9$ kJ/mol² (thin solid lines).

incongruent melting [1573–1593 K; Wyllie and Tuttle, 1960 (temperatures corrected by −32 K per Gittins and Tuttle, 1964); Irving and Wyllie, 1975], and is consistent within error with much of the liquidus equilibrium data for 1 bar (Førland, 1955). As discussed below, some liquidi at 1 bar are consistent with T_{fus}(calcite) = 1463 K.

Heat of melting

High pressure. The locations of calcite-saturated liquidi at high pressure (500–1000 bars) imply that $\Delta\overline{H}^0_{fus}$(calcite) = 31.5 ± 1 kJ/mol. This value is constrained most closely by the location of the calcite-saturated liquidus in the system $CaCO_3$-CaF_2-$BaSO_4$ (Kuellmer et al., 1966), and is consistent with all available determinations of calcite-saturated liquidi at high pressure, in which calcite is a pure phase.

The experimental location of the calcite-saturated liquidus in the system $BaSO_4$-$CaCO_3$-CaF_2 (Fig. 1, Table 3; Kuellmer et al., 1966) is the most restrictive available constraint on $\Delta\overline{H}^0_{fus}$(calcite). Calcite grown in this system is effectively pure; it does not accept significant SO_4^{2-} of F^- in solid solution, and Kuellmer et al. (1966) reported no indication of solid solution with Ba. To retrieve $\Delta\overline{H}^0_{fus}$(calcite) from this system, one substitutes Temkin melt activity models (Eq. 5) for individual anion and cation solutions into Equation 8 and then substitutes the resultant melt activity model into Equation 7, the description of the liquidus surface. The anion interaction parameters $W_{CO_3^{2-}\text{-}F^-}$, $W_{SO_4^{2-}\text{-}F^-}$, and $W_{CO_3^{2-}\text{-}SO_4^{2-}}$ are approximately zero (derived below, viz., Table 4), so Equation 8 reduces to

Table 3. Expressions for ordinate Q values in Figs. 1 and 2

$$Q1 = -RT\ln(X_{Ca^{2+},\text{cation melt}} \cdot X_{CO_3^{2-},\text{anion melt}}) \Big/ \left(1 - \frac{T}{T_{fus}}\right)$$

$$Q2 = -RT\ln(X_{Ca^{2+},\text{cation melt}}) \Big/ \left(1 - \frac{T}{T_{fus}}\right)$$

$$Q3 = -RT\ln(X_{OH^-,\text{anion melt}}) \Big/ \left(1 - \frac{T}{T_{fus}}\right)$$

$$Q4 = -RT\ln(X_{F^-,\text{anion melt}}) \Big/ \left(1 - \frac{T}{T_{fus}}\right)$$

$$Q5 = -\left[RT\ln(X_{Ca^{2+},\text{cation melt}}) - RT\ln(a_{CaCO_3,\text{calcite}})\right] \Big/ \left(1 - \frac{T}{T_{fus}}\right)$$

$$Q6 = -\frac{\left[RT\ln(X_{Ca^{2+},\text{cation melt}} \cdot X_{CO_3^{2-},\text{anion melt}}) + W_{CO_3^{2-}\text{-}OH^-}(1 - X_{OH^-,\text{anion melt}})^2\right]}{(1 - T/T_{fus})}$$

$$Q7 = -\frac{\left[RT\ln(X_{Ca^{2+},\text{cation melt}} \cdot X_{CO_3^{2-},\text{anion melt}}) + W_{CO_3^{2-}\text{-}OH^-}(1 - X_{CO_3^{2-},\text{anion melt}})^2\right]}{(1 - T/T_{fus})}$$

$$-\frac{RT\ln(X_{Ca^{2+},\text{cation melt}} \cdot X_{CO_3^{2-},\text{anion melt}})}{1 - \frac{T}{T_{fus}}} = W_{Ca^{2+}\text{-}Ba^{2+}} \frac{(1 - X_{Ca^{2+},\text{cation melt}})^2}{1 - \frac{T}{T_{fus}}} + \Delta\overline{H}^0_{fus}(\text{calcite}). \quad (12)$$

The data of Kuellmer et al. (1966) are recast by this equation in Figure 1. If the Temkin regular solution model is valid, and if the anion interaction parameters are effectively zero, the liquidus surface separating the liquid-only data points (open symbols) and liquid + calcite points (filled symbols) should be representable as a straight line with slope of $W_{Ca^{2+}\text{-}Ba^{2+}}$ and a Y-axis intercept of $\Delta\overline{H}^0_{fus}$(calcite). The liquidus can in fact be represented as a straight line consistent with the error bars of all points, suggesting $\Delta\overline{H}^0_{fus}$(calcite) = 31.05 ± 0.25 kJ/mol. However, these tight error limits are dictated by a single liquid-only point (the open symbol that extends below the lines). The conservative approach taken here is to assume that point is in error and to estimate $\Delta\overline{H}^0_{fus}$(calcite) = 31.5 ± 1 kJ/mol and $W_{Ca^{2+}\text{-}Ba^{2+}} = -11 \pm 9$ kJ/mol² from the remaining points (Fig. 1). The error limits correspond to a temperature uncertainty of ±5 K and a compositional uncertainty of ±0.2 wt% in the most abundant component.

This value for $\Delta\overline{H}^0_{fus}$(calcite) is consistent with all available high-pressure determinations of liquidi saturated in pure calcite. Figure 2a–2f show many sets of calcite-saturated liquidi recast following Equation 7. Within uncertainty, all these liquidi are consistent with $\Delta\overline{H}^0_{fus}$(calcite) = 31.5 ± 1 kJ/mol. This value is essentially identical to the only independent estimate of $\Delta\overline{H}^0_{fus}$(calcite) at high

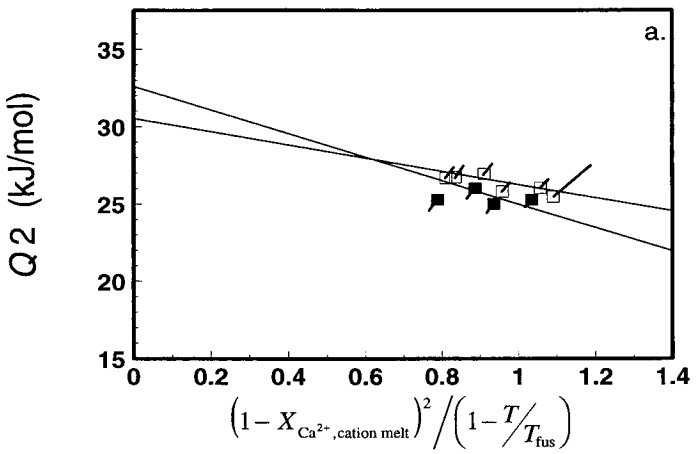

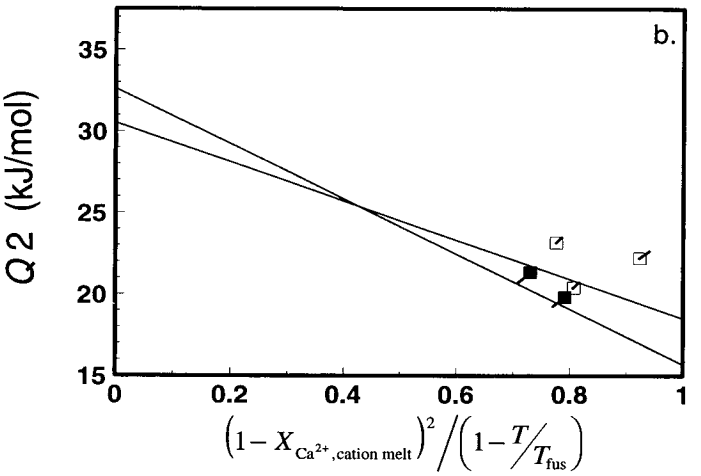

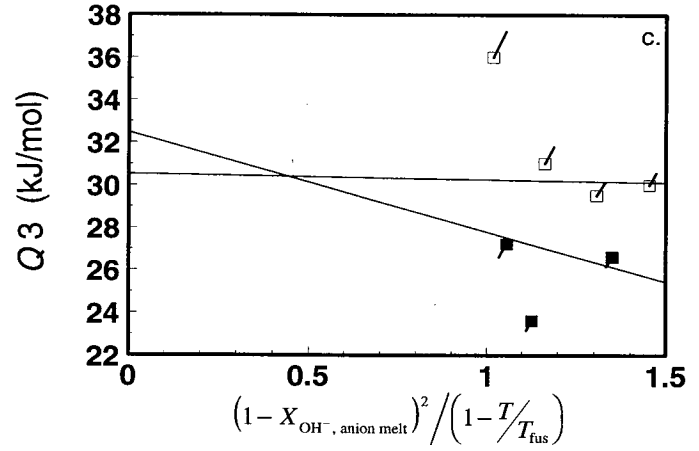

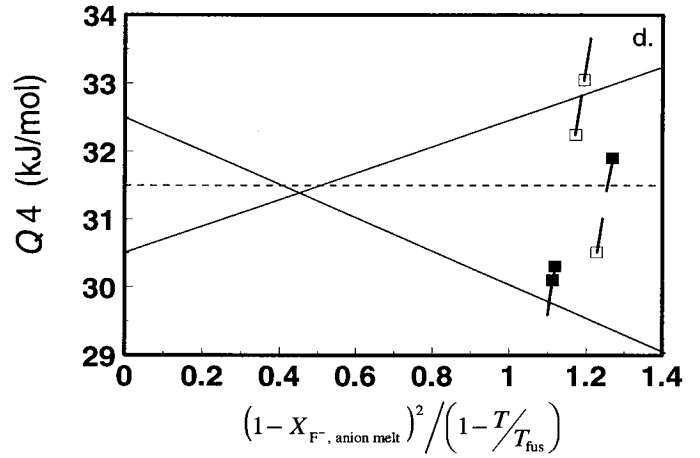

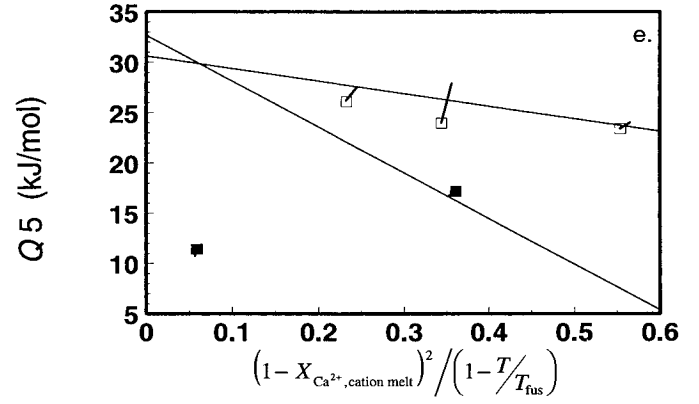

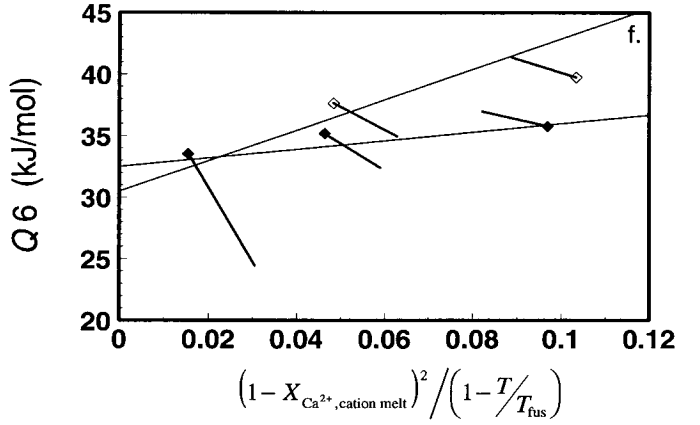

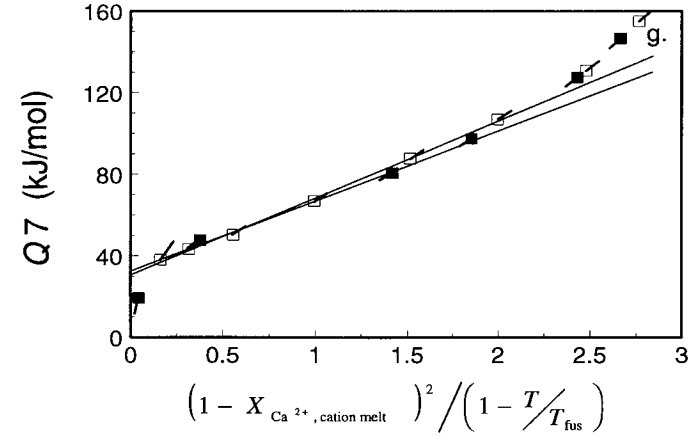

pressure, 29 kJ/mol (Bradley, 1962). Bradley assumed that 1-kbar melts in $CaCO_3$-$Ca(OH)_2$ were ideal solutions and performed an analysis of the freezing point depression similar to that here. Results here on anion solutions are consistent with near-ideal mixing of carbonate and hydroxide anions (Fig. 2c, Table 4).

One bar. Most of the limited experimental data on the melting properties of calcite at 1 bar are consistent with results from high pressure: T_{fus}(calcite) = 1583 K and $\Delta\overline{H}^0_{fus}$(calcite) = 31.5 ± 1 kJ/mol [Table 1; Flood et al.,

Fig. 2. Regular-solution interpretation of calcite-saturated liquidi from other high-pressure experiments. Open and filled symbols represent liquid-only and liquid + calcite experiments, respectively. See Table 3 for expressions of ordinate 'Q' values. Heavy lines from each data point represent a conservative estimate of errors (± 5 K in T; ± 0.2 wt% in X), showing only the error-bar halves that contribute to uncertainty in slope and intercept. The liquidus surfaces, linear with slope W and ordinate intercept of $\Delta\overline{H}^{\circ}_{fus}$(calcite), should lie between these groups of experiments. Thin solid lines encompass range of liquidus surfaces permitted by these data (with error bars), and $\Delta\overline{H}^{\circ}_{fus}$(calcite) $= 31.5 \pm 1$ kJ/mol (Fig. 1); the given range of W values is for these solid lines. (**a**) $CaCO_3$-Na_2CO_3 (1-kbar CO_2; Cooper et al., 1975), following Eq. 7. $W_{Ca^{2+}\text{-}Na^{+}} = -6 \pm 2$ kJ/mol². (**b**) $CaCO_3$-K_2CO_3 (1-kbar CO_2; Cooper et al., 1975), following Eq. 7. $W_{Ca^{2+}\text{-}K^{+}} = -14.5 \pm 2.5$ kJ/mol². (**c**) $CaCO_3$-$Ca(OH)_2$ (1-kbar CO_2; Wyllie and Tuttle, 1960; published temperatures corrected by -32 K according to Gittins and Tuttle, 1964), following Eq. 7. $W_{CO_3^{2-}\text{-}OH^{-}} = 2.3 \pm 2.3$ kJ/mol². (**d**) $CaCO_3$-CaF_2 (Gittins and Tuttle, 1964; Kuellmer et al., 1966), following Eq. 7. The data sets are not consistent within error limits; ignoring the two discrepant points (ordinate values of 30.5 and 32) permits $W_{CO_3^{2-}\text{-}F^{-}} = 0 \pm 2$ kJ/mol². (**e**) $CaCO_3$-$MgCO_3$ (10-kbar CO_2; Byrnes and Wyllie, 1981), following Eq. 6. Activities of $CaCO_3$ in calcite calculated from Anovitz and Essene (1987). $W_{Ca^{2+}\text{-}Mg^{2+}} = -40 \pm 30$ kJ/mol². (**f**) $CaCO_3$-$Ca(OH)_2$-$La(OH)_3$ (1-kbar CO_2; Jones and Wyllie, 1986), following Eq. 13. $W_{Ca^{2+}\text{-}La^{3+}} = 85 \pm 50$ kJ/mol². (**g**) $CaCO_3$-H_2O (1-kbar CO_2; Wyllie and Tuttle, 1960, temperatures corrected by -32 K according to Gittins and Tuttle, 1964), following Eq. 15. $W_{Ca^{2+}\text{-}H_2O^{+}} = 33 \pm 2$ kJ/mol².

←

1949; Førland, 1955; the location of the calcite-saturated liquidus in $CaCO_3$-Na_2CO_3 by Poletaev et al., 1975, spans too small a composition range to constrain $\Delta\overline{H}^{\circ}_{fus}$(calcite)]. However, the liquidus position in the $CaCO_3$-Na_2CO_3 system at temperatures below approximately 1170 K is consistent with T_{fus}(calcite) = 1463 K and $\Delta\overline{H}^{\circ}_{fus}$(calcite) $\approx$ 38 kJ/mol (Table 1; Flood et al., 1949; Førland, 1955). To account for these discrepancies, Førland (1955) suggested that lower temperature melts in $CaCO_3$-Na_2CO_3 do not have the same structure as higher temperature melts and melts in other systems (notably K-bearing). There is no evidence that the low-temperature structure persists to higher temperature or pressure in the Ca-rich systems examined here.

Extrapolations of T_{fus}(calcite) and $\Delta\overline{H}^{\circ}_{fus}$(calcite) from high pressure are consistent with most of the 1-bar liquidus experiments of Førland (1955), who calculated both values from the compositions of melts saturated with CaO (lime) in the systems $CaCO_3$-Na_2CO_3, $CaCO_3$-K_2CO_3, and $CaCO_3$-$NaKCO_3$ as functions of CO_2 pressure between 1203 and 1273 K. Compositions were measured by weight loss (CO_2 loss); a (calcite) was calculated from measured CO_2 pressure and the known pressure of CO_2 in equilibrium with calcite and CaO; uncertainties were not given and cannot be evaluated. The linear correlation of $\Delta\overline{G}_{fus}$ (calcite) and T for the systems $CaCO_3$-K_2CO_3 and $CaCO_3$-$NaKCO_3$ implied T_{fus}(calcite) $\approx$ 1523 K and $\Delta\overline{H}^{\circ}_{fus}$(calcite) $\approx$ 35 kJ/mol. The original data are consistent with T_{fus}(calcite) = 1583 K (extrapolated above from high-pressure equilibria), which yields $\Delta\overline{H}^{\circ}_{fus}$(calcite) $\approx$ 30.5 kJ/mol, consistent with high-pressure phase equilibria. Liquidus experiments at high Ca contents and higher temperatures in the system $CaCO_3$-Na_2CO_3, are also consistent with the high-pressure values, although data are limited.

However, at lower temperatures and lower Ca contents, the CaO-saturated liquidus in $CaCO_3$-Na_2CO_3 is not consistent with T_{fus}(calcite) and $\Delta\overline{H}^{\circ}_{fus}$(calcite) from high-pressure phase equilibria. Rather, Førland (1955) found that these liquidus determinations suggested T_{fus}(calcite) = 1463 K and $\Delta\overline{H}^{\circ}_{fus}$(calcite) $\approx$ 37.5 kJ/mol.

This higher $\Delta\overline{H}^{\circ}_{fus}$(calcite) and lower T_{fus}(calcite) are also consistent with the earlier liquidus experiments of Flood et al. (1949). They determined the CaO-saturated liquidus surfaces in $CaCO_3$-Na_2CO_3, $CaCO_3$-K_2CO_3, and $CaCO_3$-Li_2CO_3 under 1 bar CO_2, from 1244 to 1378 K. Activities of calcite in the melt solutions were calculated from the pressure of CO_2 in equilibrium with calcite and lime; uncertainties were given only as error bars on graphs and cannot be readily evaluated. Flood et al. (1949) took the melting temperature for calcite to be 1613 K, used a molecular mole fraction model for melt activities, and calculated (from Eq. 7) that $\Delta\overline{H}^{\circ}_{fus}$(calcite) = 14.2 kJ/mol. Recalculating their data for $CaCO_3$-Na_2CO_3 for melting temperatures of 1583 or 1463 K and with a Temkin melt model (e.g., ionic fractions) yields $\Delta\overline{H}^{\circ}_{fus}$(calcite) $\approx$ 39 kJ/mol, consistent with Førland's (1955) data on Ca-poor compositions in $CaCO_3$. The determinations for $CaCO_3$-K_2CO_3 and $CaCO_3$-Li_2CO_3 of Flood et al. (1949) are more scattered and are consistent with either pair of T_{fus}(calcite) and $\Delta\overline{H}^{\circ}_{fus}$(calcite).

To explain the discrepancies in $\Delta\overline{H}^{\circ}_{fus}$(calcite) and T_{fus}(calcite), Førland (1955) suggested that the more Na-rich and lower-temperature melts in $CaCO_3$-Na_2CO_3 have a different structure from those at higher Ca contents and temperatures. On the basis of the $\Delta\overline{H}_{fus}$(calcite) values, the Ca-rich melt structure is present in all systems at high pressure. Another speculative explanation is that the solid in the $CaCO_3$-Na_2CO_3 experiments was not actually CaO but a mixed oxide phase in CaO-Na_2O. I am aware, however, of no reports of mixed Na-Ca oxide phases.

Melt volume

The volume change on melting calcite at high pressure may be calculated from Equation 9. The entropy of fusion, $\Delta\overline{S}_{fus}$(calcite), is calculated from $\Delta\overline{H}^{\circ}_{fus}$(calcite) and T_{fus}(calcite), as in Table 2. The slope of the polybaric congruent melting for calcite curve is 80 K/bar (Irving and Wyllie, 1973, 1975), yielding $\Delta\overline{V}_{fus}$(calcite) = 2.5 $\pm$ 0.1 cm³/mol at high pressure. This value is comparable with $\Delta\overline{V}_{fus}$ for Li_2CO_3, but significantly smaller than those for K_2CO_3 and Na_2CO_3 (Table 2).

The molar volume of $CaCO_3$ melt could now be esti-

TABLE 4. Mixing of ions in molten salts: Regular solution parameters

Ions	W (kJ/mol²)	Counter ion	Reference
CO_3^{2-}-OH^-	-2.3 ± 2.3	Ca^{2+}	1
	~0	Na^+	2
CO_3^{2-}-F^-	0 ± 2	Ca^{2+}	1
	~−2	K^+	3
CO_3^{2-}-Cl^-	−1.7, 0	Na^+	3, 4
CO_3^{2-}-Br^-	−1.7	Na^+	4
CO_3^{2-}-SO_4^{2-}	0	Na^+	5
	0 ± 1.5	Ca^{2+}	1
CO_3^{2-}-PO_4^{3-}	>65?	Ca^{2+}	1
CO_3^{2-}-O^{2-}	~0	Na^+	2
CO_3^{2-}-O_2^{2-}	~0	Na^+	2
F^--OH^-	+4.3	Ca^{2+}	6
F^--SO_4^{2-}	~0	Na^+	7
Ca^{2+}-Na^+	-6 ± 2	CO_3^{2-}	1
	~−10	CO_3^{2-}	8
Ca^{2+}-K^+	-14.5 ± 2.5	CO_3^{2-}	1
	~−24	CO_3^{2-}	8
Ca^{2+}-Li^+	−2.5	CO_3^{2-}	4
Ca^{2+}-H_3O^+	36 ± 2	CO_3^{2-}-OH^-	1
Ca^{2+}-Mg^{2+}	-40 ± 20	CO_3^{2-}	1
Ca^{2+}-Ba^{2+}	-11 ± 9	CO_3^{2-}-SO_4^{2-}	1
Ca^{2+}-La^{3+}	$+85 \pm 50$	CO_3^{2-}-OH^-	1
Mg^{2+}-K^+	-20 ± 30?	CO_3^{2-}	1
Na^+-K^+	−5.6	CO_3^{2-}	9
Na^+-Li^+	−11.2	CO_3^{2-}	9

Note: 1 = this work; 2 = Selman and Maru (1981); 3 = from phase diagrams in Levin et al. (1964, 1969); 4 = Lumsden (1966); 5 = Flood et al. (1952); 6 = average value from Tacker and Stormer (1993); 7 = average value from Kleppa and Julsrud (1980); 8 = Førland (1955) and recalculation of Flood et al. (1949); 9 = average value from Andersen and Kleppa (1976).

mated from this if the molar volume of solid $CaCO_3$ were known. At its 1-kbar melting temperature, $CaCO_3$ would be in the $CaCO_3$ (V) polymorph (Carlson, 1983); unfortunately, molar volumes have been measured only to 1148 K and 1 bar, where $CaCO_3$ (V) is the stable polymorph (Mirwald, 1979). Recklessly extrapolating molar volume and compressibility data for $CaCO_3$ (IV) (Mirwald, 1979) to 1583 K and 1 kbar, I estimate a molar volume for solid $CaCO_3$ of 39 cm³/mol. This value leads to a molar volume for liquid $CaCO_3$ of 41.5 cm³/mol and a density of 2.4 gm/cm³. This density is comparable with the 2.2 gm/cm³ inferred for a Ca-rich carbonatite magma (Nesbitt and Kelly, 1977).

Structures of $CaCO_3$-rich melts

For modeling Ca-rich carbonate melt systems, it seems reasonable to accept $\Delta\overline{H}_{fus}$(calcite) and T_{fus}(calcite) from the 1-kbar experiments (Table 2) and as extrapolated to other pressures (Table 1). There are no obvious problems with experiments or interpretation to explain the differences between the inferences from high-pressure phase equilibria and the results of Flood et al. (1949) and some results of Førland (1955). It is quite reasonable to infer, as did Førland (1955), that carbonate melts at low pressure can adopt multiple structures. The structure obtained at high pressure (1 kbar) seems to be retained at 1 bar for compositions rich in Ca and those containing significant K; for these melts, $\Delta\overline{H}^0_{fus}$(calcite) = 31.5 ± 1 kJ/mol and T_{fus}(calcite) = 1583 K. For melts relatively rich in Na at low pressure and relatively lower temperature, $\Delta\overline{H}^0_{fus}$(calcite) ~ 38.5 kJ/mol, and T_{fus}(calcite) = 1463 K. On the basis of molar entropies, one may speculate that the former melts are structurally comparable to molten K_2CO_3 and the latter are structurally comparable with molten Na_2CO_3.

MAGNESIUM CARBONATE

The common presence of magnesian calcite, dolomite, and magnesian silicates in carbonatites shows that magnesium carbonate is an important component in carbonatite petrogenesis. Unfortunately, data on the melting and thermophysical properties of magnesium carbonate are either absent or uncertain. Dolomite, $CaMg(CO_3)_2$, is the most common Mg-bearing carbonate in carbonatites, but it decarbonates at low pressure and melts incongruently at high pressure. In addition, there appear to be no available liquidus equilibria that can be used as above to derive its melting properties. Data on Mg in carbonate melts must now come from the limited studies available involving $MgCO_3$, magnesite.

Magnesite melts incongruently at pressures below 25 kbar, and the hypothetical congruent melting temperature must be extrapolated from there to the range of interest. Using the high-pressure liquidus determinations of Irving and Wyllie (1975), the 1 kbar congruent melting temperature for $MgCO_3$ may be extrapolated as 1753 K.

The $\Delta\overline{H}^0_{fus}$(magnesite) is very poorly determined by the single available liquidus location, in $MgCO_3$-K_2CO_3 (Ragone et al., 1966), for which magnesite is not a solid solution. Taken at face value, the brackets of Ragone et al. (1966) on the magnesite-saturated liquidus surface only restrict $\Delta\overline{H}^0_{fus}$(magnesite) to a value of 32 ± 25 kJ/mol and (Table 2), with a corresponding entropy of fusion of 18 ± 15 J/(mol·K) (Table 2) and a $W_{Mg^{2+}\text{-}K^+}$ of −20 ± 30 kJ/mol². However, including reasonable experimental uncertainties in the analysis (5 K and 0.2 mol% $MgCO_3$) only restricts $\Delta\overline{H}^0_{fus}$(magnesite) to >7 kJ/mol and $W_{Mg^{2+}\text{-}K^+}$ to <10 kJ/mol². Clearly, much work remains.

THERMOCHEMISTRY OF SOLUTION

In the regular-solution model, there is a heat effect in the formation of a solution, but no entropy effect beyond that of random mixing of constituents (Eq. 4; viz., Lewis and Randall, 1961). The heat effect is described by a single interaction parameter, W, for each possible pair (or multiplet) of species in a solution. For a Temkin ionic solution, there are independent Ws for the cation and anion solutions. The regular solution parameters W are obtained simultaneously with estimates of $\Delta\overline{H}_{fus}$, and so have already appeared above in discussions of Figures 1, 2, and 3.

Anion mixing

It is likely that the anion solution of carbonatite magmas is dominated by the carbonate anion, but other anions may play an important or essential role in carbonate petrogenesis. For instance, the presence of OH anions

permits carbonate-rich magmas to melt at geologically reasonable temperatures (Wyllie and Tuttle, 1960; Wyllie, 1989), and fluoride anions are inferred to have an equally large effect on liquidus phase relations (Gittins et al., 1990; Jago and Gittins, 1991).

The anion solutions (Temkin model) in carbonate-rich melts are nearly ideal for all nonpolymerizing anions (Table 4): ". . . mixed anion–common cation fused salts often are very nearly ideal solutions" (Kleppa and Julsrud, 1980). Data are available from Ca-rich and some other binary systems on the interaction of carbonate anions with fluoride and other halide, hydroxide, oxide, peroxide, and sulfate ions (Table 4). W values constrained here include those for CO_3^{2-}-OH^- (Fig. 2c) and CO_3^{2-}-F^- (Fig. 2d). Values of W in Table 4 for all anion solutions except carbonate-orthophosphate are near zero, confirming their nearly ideal behavior.

Mixing of sulfate and carbonate in ionic melts appears essentially ideal. Flood et al. (1952) studied melts in the system Na_2CO_3-Na_2SO_4-CO_2 for electrochemical applications, and found that the melts behaved as ideal solutions. The ideality of carbonate-sulfate mixing extends to Ca-rich compositions, as the calcite-saturated liquidus surface in $CaCO_3$-$CaSO_4$ at 1 bar (Fuerstenau et al., 1981) is consistent with $W_{CO_3^{2-}\text{-}SO_4^{2-}} = 0$ kJ/mol², if $\Delta\overline{H}^0_{fus}$(calcite) = 31.5 kJ/mol (Fig. 3).

Mixing properties of carbonate and sulfide anions would be very useful in understanding redox states of natural systems and in some carbonatite-hosted ore deposits, but no definitive data are available. The liquidus location in $CaCO_3$-$Ca(OH)_2$-CaS at 1 kbar by Helz and Wyllie (1979) cannot be interpreted uniquely here because $W_{S^{2-}\text{-}OH^-}$ is not known. Their data on the binary join $Ca(OH)_2$-CaS and estimates of the melting temperature and heat of fusion for CaS suggest that $W_{S^{2-}\text{-}OH^-}$ is approximately +15 kJ/mol²; this value is obviously suspect. The liquidus location in $CaCO_3$-$CaSO_4$-CaS determined at low pressure by Fuerstenau et al. (1981) cannot be interpreted unambiguously here because $W_{S^{2-}\text{-}SO_4^{2-}}$ is not known. However, if $W_{S^{2-}\text{-}SO_4^{2-}}$ is taken as zero, $W_{S^{2-}\text{-}CO_3^{2-}}$ must be near +100 kJ/mol.

The behavior of phosphate may be far from ideal. The mixing of carbonate and orthophosphate (PO_4^{3-}) anions was suggested to be nearly ideal by analogy with the mixing of carbonate and sulfate anions (Table 4; Treiman, 1989). However, Tacker and Stormer (1993) have shown that solutions of molten calcium orthophosphate and other calcium salts (hydroxide, chloride, and fluoride) are not ideal, with regular-solution interaction parameters more negative than −20 kJ/mol². They suggested further that carbonate-orthophosphate mixing might also be nonideal. The data of Biggar (1969) appear to be the only liquidus determinations relevant to the mixing of alkaline earth carbonates and phosphates. His experiments yielded only a single bracket on the calcite-saturated liquidus in a system containing orthophosphate. Taken at face value, this liquidus bracket suggests $W_{CO_3^{2-}\text{-}PO_4^{3-}} \approx +65$ kJ/mol², assuming a symmetrical regular solution, $\Delta\overline{H}^0_{fus}$(calcite) = 31.5 kJ/mol (Table 2), $W_{CO_3^{2-}\text{-}OH^-} = -2.3$ kJ/mol² (Table 4), and $W_{PO_4^{3-}\text{-}OH^-} \cong -27$ kJ/mol² (calculated from Table 4 of Tacker and Stormer, 1933). However, Biggar (1969) suggested that these experiments may be faulty and that the liquidus may lie at even higher temperatures, in which case $W_{CO_3^{2-}\text{-}PO_4^{3-}}$ would be even larger. Such a large positive $W_{CO_3^{2-}\text{-}PO_4^{3-}}$ implies that some carbonate-rich and phosphate-rich melts might be immiscible. In nature, phosphate-rich segregations (called phoscorite or camaforite) are common in some carbonatites (e.g., Eriksson, 1989), and it has been suggested they form by carbonate-phosphate liquid immiscibility (Lapin, 1976). Continued experimentation will be required to understand the thermochemistry of phosphate-carbonate mixing.

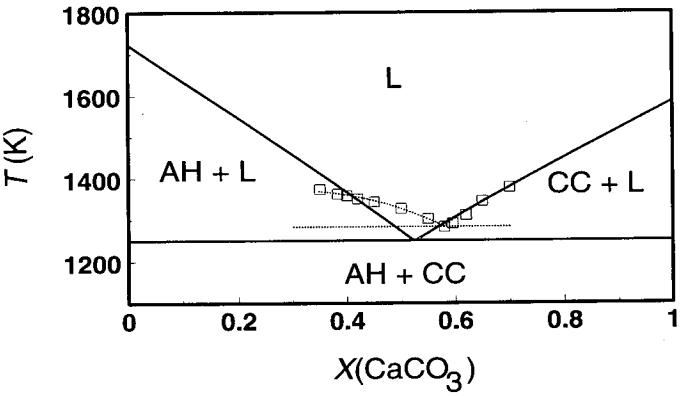

Fig. 3. Liquidus phase diagrams for $CaCO_3$-$CaSO_4$: phases are CC, calcite ($CaCO_3$); AH, anhydrite ($CaSO_4$), not including polymorphic transitions; and L, liquid. Solid lines are as predicted by the regular-solution model (Eq. 7) and ideal mixing of CO_3^{2-} and SO_4^{2-} (Table 4) for a total pressure of ~100 bars. Open squares and dotted lines are experimental determinations of the liquidus and solidus by differential thermal analysis (Fuerstenau et al., 1981). Predicted and experimental positions of the calcite-saturated liquidus agree within error. The experimentally determined position of the anhydrite-saturated liquidus is not consistent with the predicted liquidus and does not extrapolate to the known melting temperature of anhydrite. Since Fuerstenau et al. (1981) did not characterize their experiment products, it is possible that their liquidus surface represents growth of a mixed anion solid that melts incongruently.

There are few quantitative data on the mixing behavior of carbonate and silicate anions in carbonate melts. The mixing of carbonate with orthosilicate (SiO_4^{4-}) may be close to ideal (Treiman, 1989). However, the limited data available (in the system CaO-SiO_2-CO_2-H_2O: Wyllie and Haas, 1965) are difficult to interpret because the proportions and speciations of H_2O in the melts are not known. Mixing of carbonate anions with more polymerized aluminosilicate anions is far from ideal, as shown by the immiscibility of carbonate and silicate melts. This liquid immiscibility covers a wide range of synthetic and natural compositions (e.g., Koster van Groos and Wyllie, 1966; Treiman and Essene, 1985; Kjarsgaard and Hamilton, 1989). Even in compositions without immiscibility, car-

bonate anions tend to form clusters that exclude polymerized silicate anions (Mysen and Virgo, 1980). The degree of this nonideality is a function of the composition of the silicate melt (Mysen and Virgo, 1980; Fine and Stolper, 1985) and remains to be characterized fully.

Cation mixing

Within the accuracy limits of available data, cation mixing in Ca-rich carbonate melts is adequately described by the regular-solution model. The regular-solution parameters W in Table 4 are taken from the literature and developed here (Figs. 1, 2a–2b, 2e–2f, and 3). Regular-solution interaction parameters for Ca^{2+} and monovalent and divalent cations tend to be moderate and negative, suggesting the association of unlike cations in the melt. The only value for a trivalent cation, La^{3+}, is large and positive.

Alkali cations. The interaction parameters W for Ca-Na and Ca-K carbonate systems at high pressure (Table 4) were derived in concert with $\Delta\overline{H}^{0}_{fus}$(calcite) from data of Cooper et al. (1975) in Figure 2a and 2b. The $W_{Ca^{2+}\text{-}K^{+}}$ value for 1 bar are significantly higher (Table 4, based on Flood et al., 1949, and Førland, 1955); the source of the discrepancy is unknown. A Ca^{2+}-Li^{+} interaction parameter is available in the literature (Lumsden, 1966). The $W_{Na^{+}\text{-}K^{+}}$ and $W_{Na^{+}\text{-}Li^{+}}$ of Table 4 are averages from the data of Andersen and Kleppa (1976); their precise calorimetry showed that both values are slight functions of composition across the respective joins.

Alkaline earth cations. Very few data are available for the estimation of solution parameters for alkaline earths (besides Ca) in carbonate melts. The value for $W_{Ca^{2+}\text{-}Ba^{2+}}$ was defined in Figure 1 during determination of $\Delta\overline{H}^{0}_{fus}$(calcite).

To estimate the W interaction parameter for the Ca^{2+}-Mg^{2+} cation solution in carbonate melts, Equation 6 and the activity-composition model of Anovitz and Essene (1987) can be applied to the liquidus phase equilibria of Byrnes and Wyllie (1981). Figure 2e shows that liquidus, with the range of permissible liquidus locations forced through $\Delta\overline{H}^{0}_{fus}$(calcite) = 31.5 ± 1 kJ/mol on the vertical axis. The permissible liquidus locations correspond to $W = -40 \pm 30$ kJ/mol. This result must be used with caution because the liquidus of Byrnes and Wyllie (1981) was determined at 10 kbar; the activity-composition model has been extrapolated somewhat beyond its known range of applicability, and the validity of the activity model is in question (McSwiggen, 1993). As a further caution, a similar analysis performed on the 27-kbar liquidus in $CaCO_3$-$MgCO_3$ (Irving and Wyllie, 1975) is consistent with a regular solution W of approximately zero. Obviously, data in this system are too sparse for firm conclusions, but changes in melt structures are possible.

Other cations. Interpretable liquidus data for other cations in carbonate melts are limited to lanthanum in the system $CaCO_3$-$Ca(OH)_2$-$La(OH)_3$ (Jones and Wyllie, 1986). As calcite accepts little OH^- or La^{3+} in solid solution, the calcite-saturated liquidus may be modeled as

$$-\left\{[RT\ln(X_{Ca^{2+},\text{cation melt}}\cdot X_{CO_3^{2-},\text{anion melt}}) + W_{CO_3^{2-}\text{-}OH^-}(1 - X_{CO_3^{2-},\text{anion melt}})^2]\Big/\left(1 - \frac{T}{T_{fus}}\right)\right\} = W_{Ca^{2+}\text{-}La^{3+}}\frac{(1 - X_{Ca^{2+},\text{cation melt}})^2}{1 - \frac{T}{T_{fus}}} + \Delta\overline{H}^{0}_{fus}(\text{calcite}) \quad (13)$$

following Equations 7 and 12. This equation is in the format $y = ax + b$; when it is graphed in that manner, experimental brackets on the calcite-saturated liquidus ought to permit it to be a straight line with a slope of $W_{Ca^{2+}\text{-}La^{3+}}$ and an intercept of $\Delta\overline{H}^{0}_{fus}$(calcite) = 31.5 ± 1 kJ/mol. The limited data are consistent with regular-solution behavior and $W_{Ca^{2+}\text{-}La^{3+}} = +80 \pm 50$ kJ/mol² (Fig. 2f, Table 4).

Solution of H_2O

H_2O is important, both as a flux to permit melting of carbonates at geologically reasonable conditions (Wyllie and Tuttle, 1960) and as a constituent of the vapors associated with carbonatites (e.g., Rankin, 1975; Nesbitt and Kelly, 1977; McKie, 1966; LeBas, 1977; Rubie and Gunter, 1983). H_2O is problematic within an ionic melt model as it is not an ionic liquid. Further, the speciation of H_2O in ionic solutions may be affected by cation complexation, formation of mixed anions (like bicarbonate), and changes in intrinsic variables (like acidity and f_{O_2}). In addition, H_2O does not behave as OH does in carbonate-rich ionic melts; the calcite-saturated liquidus in $CaCO_3$-$Ca(OH)_2$ is effectively straight and not inflected, whereas the calcite-saturated liquidus in $CaCO_3$-H_2O is strongly curved and inflected, concave up at high $CaCO_3$ contents, and concave down at lower $CaCO_3$ contents (Figs. 5 and 6, respectively, of Wyllie and Tuttle, 1960).

Even so, the solution of H_2O in Ca-carbonate melts can be described with a simple regular-solution model, on the basis of the liquidus surface in the system $CaCO_3$-H_2O (Wyllie and Tuttle, 1960, temperatures corrected by −32 K per Gittins and Tuttle, 1964). I will assume that H_2O ionizes completely into hydroxide and hydronium ions on solution in a carbonate melt:

$$2H_2O \rightleftharpoons H_3O^+ + OH^- \quad (14)$$

and so affects both the cation and anion solutions directly. The experiments of Wyllie and Tuttle (1960) were done with excess vapor in most cases; because the composition of the vapor is unconstrained, I must assume further that the mass of vapor was insignificant compared with that of the solid (i.e., that the mass of H_2O input to the charge effectively represents the mass of H_2O in the liquid). With this speciation model, Equations 5 and 7 can be combined and reduced to yield

$$-\left\{[RT\ln(X_{Ca^{2+},\text{cation melt}}\cdot X_{CO_3^{2-},\text{anion melt}}) + W_{CO_3^{2-}\text{-}OH^-}(1 - X_{CO_3^{2-},\text{anion melt}})^2]\Big/\left(1 - \frac{T}{T_{fus}}\right)\right\} = W_{Ca^{2+}\text{-}H_3O^+}\frac{(1 - X_{Ca^{2+},\text{cation melt}})^2}{1 - \frac{T}{T_{fus}}} + \Delta\overline{H}^0_{fus}(\text{calcite}) \quad (15)$$

comparable with Equation 13 above. $X_{Ca^{2+},\text{cation melt}}$ and $X_{CO_3^{2-},\text{anion melt}}$ have the same numerical values, because they both arise from disproportionation of H_2O. Constraints on the calcite-saturated liquidus in $CaCO_3$-H_2O from Wyllie and Tuttle (1960) are recast in Figure 2g in this form, with the term in brackets on the ordinate and the term attached to $W_{Ca^{2+}\text{-}H_3O^+}$ on the abscissa. $W_{CO_3^{2-}\text{-}OH^-}$ is from Table 4. For the model to be correct, the liquidus surface must be representable as a straight line, with an ordinate intercept of $\Delta\overline{H}^0_{fus}$(calcite) = 31.5 ± 1 kJ/mol and a slope of $W_{Ca^{2+}\text{-}H_3O^+}$. Figure 2g shows that these criteria are met for the ten experiments at lower abscissa values, which have <40 wt% H_2O (equivalent to $X_{H_2O} \leq 0.9$). To match these experiments, $W_{Ca^{2+}\text{-}H_3O^+} = 36 \pm 2$ kJ/mol², which is high but not unreasonable compared with other W values (Table 4).

It remains unclear how closely this model cleaves to reality. Instead of a straight line in Figure 2g, one could also fit a smooth curve through all the liquidus brackets, inconsistent with regular solution behavior. It is entirely possible that effects of formation of complexes, formation of mixed anions, or violation of other assumptions are hidden in the correlation of Figure 2g. If accurate, however, it suggests that dissolved H_2O at high temperatures in ionizing environments behaves as the ionic compound hydronium hydroxide, $H_3O^+OH^-$. These hypotheses about H_2O in carbonate magmas should be readily testable.

Applications

Beyond the value of a theoretical understanding of carbonatite magmas, this regular-solution model can help answer real geological questions involving carbonate melts. Here, two types of questions are considered: the relationships between the compositions of carbonatite magmas and their vapors and the prediction of liquidus equilibria.

Carbonatite magma and vapor

A fluid or vapor phase is commonly associated with carbonatites, as shown by their fluid inclusions (e.g., Rankin, 1975; Nesbitt and Kelly, 1977) and surrounding metasomatic rocks (fenites: e.g., McKie, 1966; LeBas, 1977; Rubie and Gunter, 1983). An understanding of the vapor phase is important for understanding the application of experimental phase equilibria to natural carbonatites, the origins of carbonatite metasomatism, and the effects of volatile loss or gain on magma composition. Because the vapor phase is fugitive, its composition is elusive. In rare cases, its composition can be constrained by the mineral assemblage of the carbonatite (Treiman and Essene, 1984), but not without dispute (Gittins et al., 1990, 1992; Treiman and Essene, 1992).

A solution model for carbonate-rich melts provides a link between carbonatite magmas and vapors. From the composition of a carbonatite magma (e.g., its halogen content), a solution model permits calculation of some compositional constraints on the vapor in equilibrium with the magma. Alternatively, given the composition of a vapor phase (e.g., its H_2O content), one can constrain the composition of the magma.

F: Experimental calibration. Carbonatite magmas can contain significant F. Most carbonatites contain fluorapatite and some carry fluorite (CaF_2); many other F-bearing minerals may be present, e.g., pyrochlore, fluocerite [(Ce,La)F_3], bastnaesite [(Ce,La)(CO_3)F], and amphiboles (Hogarth, 1989). The natrocarbonatites of Oldoinyo Lengai, Tanzania, also contain F-bearing nyerereite [$(Na,K)_2Ca(CO_3)_2$], and gregoryite [$(Na_2,Ca)CO_3$] (Peterson, 1990). Many fenites associated with carbonatites contain fluorite, some in economic proportions. In addition, theoretical interest has recently focused on F because of the experimental observation that F is similar to H_2O as a flux to permit melting of carbonates at geologically reasonable temperatures (Gittins et al., 1990; Jago and Gittins, 1991).

The behavior of F in carbonatite magma-vapor systems can be modeled by the reaction

$$\underset{\text{vapor}}{F_2} + \underset{\text{melt}}{CO_3^{2-}} \rightleftharpoons \underset{\text{melt}}{2F^-} + \underset{\text{vapor}}{CO_2} + \underset{\text{vapor}}{\tfrac{1}{2}O_2} \quad (16)$$

which describes the equilibrium distribution of F between carbonate melt and vapor. To calibrate the distribution of F, one must derive the standard Gibbs free energy of Reaction 16 in the temperature range of interest (ignoring the effects of pressure on melt components),

$$\Delta\overline{G}^0_r = -RT\ln\left(\frac{f_{CO_2,\text{vapor}}\cdot f^{1/2}_{O_2,\text{vapor}}}{f_{F_2,\text{vapor}}}\cdot\frac{a^2_{F^-,\text{melt}}}{a_{CO_3^{2-},\text{melt}}}\right) \quad (17)$$

where each a is the activity of a melt component and each f is the fugacity of a vapor species. If all the fugacities and activities can be determined at a given temperature, the free energy of reaction is readily calculated.

The Gibbs energy of Equation 17 can be calculated along the calcite + fluorite saturated liquidus in the system CaF_2-$Ca(OH)_2$-$CaCO_3$, as drawn by Gittins and Tuttle (1964) from their 1-kbar experimental results (their Fig. 4). The ratio of gas species fugacities in Equation 17 is buffered by the presence of solid calcite and fluorite,

$$\underset{\text{vapor}}{F_2} + \underset{\text{solid}}{CaCO_3} \rightleftharpoons \underset{\text{solid}}{CaF_2} + \underset{\text{vapor}}{CO_2} + \underset{\text{vapor}}{\tfrac{1}{2}O_2}. \quad (18)$$

Activities of melt species come directly from the analyzed or inferred compositions of the melts, and activity coef-

ficients come from the melt solution model. With $W_{OH^-\text{-}F^-\text{-}CO_3^{2-}}$ and $W_{F^-\text{-}CO_3^{2-}}$ as zero (Table 4), activity coefficients are given as

$$RT \ln \gamma_{CO_3^{2-}} = W_{CO_3^{2-}\text{-}OH^-}(X_{OH^-}^2 + X_{F^-}X_{OH^-}) - W_{F^-\text{-}OH^-}(X_{F^-}X_{OH^-}) \quad (19a)$$

and

$$RT \ln \gamma_{F^-} = W_{F^-\text{-}OH^-}(X_{OH^-}^2 + X_{CO_3^{2-}}X_{OH^-}) - W_{CO_3^{2-}\text{-}OH^-}(X_{CO_3^{2-}}X_{OH^-}) \quad (19b)$$

from Equation 5. To obtain $\Delta\overline{G}_r^0$ in Equation 17, the gas fugacity ratio is calculated using thermochemical data from Chase et al. (1974) and Robie et al. (1979), and melt component activities are calculated from measured or inferred melt compositions (Gittins and Tuttle, 1964) and activity coefficients (Eq. 19), with W values from Table 4. Taking seven points from the liquidus of Gittins and Tuttle (1964) from 1153–848 K yielded a regressed free energy equation of

$$\Delta\overline{G}_r^0 = -412.0\ (\pm 2.8) - 0.091\ (\pm 0.003)T\ \text{(kJ/mol)} \quad (20)$$

with $r^2 = 0.995$, where the uncertainties are the 2σ standard errors of regression. If the regular-solution model here is accurate, this calibration should be valid for all Ca-rich carbonate-rich melts, whether in synthetic or complex natural systems. The free energies of reaction are negative and imply that Reaction 16 favors strongly the production of fluoride ions and carbon dioxide gas. Thus, the vast proportion of F in Ca-rich carbonatite melt-vapor systems is in the melt, and the vapor contains little F (Treiman and Essene, 1992).

Hydroxide: Experimental calibration. Carbonatite magmas may contain significant H_2O, as suggested by Wyllie and Tuttle (1960) to explain how carbonate-rich melts might form at reasonable geological temperatures. Since that time, the importance of H_2O as a flux in carbonatite magmas has gained wide acceptance, although some experiments suggest that F may be equally effective as a flux (Gittins et al., 1990; Jago and Gittins, 1991).

The exchange of H_2O and OH between carbonatite magma and vapor systems can be modeled, in the same manner as F above, by the reaction

$$\underset{\text{vapor}}{H_2O} + \underset{\text{melt}}{CO_3^{2-}} \rightleftharpoons \underset{\text{melt}}{2OH^-} + \underset{\text{vapor}}{CO_2}. \quad (21)$$

Unlike the case for F, there is no dependence here on f_{O_2}. Calibration of this equilibrium requires derivation of its standard Gibbs free energy in the temperature range of interest (if one ignores the effects of pressure on melt components),

$$\Delta\overline{G}_r^0 = -RT \ln\left(\frac{f_{CO_2,\text{vapor}}}{f_{H_2O,\text{vapor}}} \cdot \frac{a_{OH^-,\text{melt}}^2}{a_{CO_3^{2-},\text{melt}}}\right) \quad (22)$$

where each a is the activity of a melt component and each f is the fugacity of a vapor species. The Gibbs energies of Reaction 21 can be calculated for compositions along the calcite + portlandite [$Ca(OH)_2$]-saturated liquidus in the system CaF_2-$Ca(OH)_2$-$CaCO_3$ (Gittins and Tuttle, 1964), the same data set used for calibration of the carbonate + fluorine exchange above. The ratio of gas species fugacities in Equation 22 is buffered by the presence of solid calcite and portlandite and the equilibrium

$$\underset{\text{vapor}}{H_2O} + \underset{\text{solid}}{CaCO_3} \rightleftharpoons \underset{\text{solid}}{Ca(OH)_2} + \underset{\text{vapor}}{CO_2}. \quad (23)$$

Activities of melt species are calculated from analyzed or inferred melt compositions and regular-solution activity coefficients. With $W_{OH^-\text{-}F^-\text{-}CO_3^{2-}}$ and $W_{F^-\text{-}CO_3^{2-}}$ as zero (Table 4), activity coefficients are given as

$$RT \ln \gamma_{CO_3^{2-}} = W_{CO_3^{2-}\text{-}OH^-}(X_{OH^-}^2 + X_{F^-}X_{OH^-}) - W_{F^-\text{-}OH^-}(X_{F^-}X_{OH^-}) \quad (24a)$$

and

$$RT \ln \gamma_{OH^-} = W_{F^-\text{-}OH^-}(X_{F^-}^2 + X_{CO_3^{2-}}X_{F^-}) + W_{CO_3^{2-}\text{-}OH^-}(X_{CO_3^{2-}}^2 + X_{CO_3^{2-}}X_{F^-}) \quad (24b)$$

from Equation 5. To obtain $\Delta\overline{G}_r^0$ in Equation 22, the gas fugacity ratio is calculated using thermochemical data from Chase et al. (1974) and Robie et al. (1979), and melt component activities are calculated from measured melt compositions (Gittins and Tuttle, 1964). Activity coefficients (Eqs. 24a and 24b) using W values are from Table 4. The calcite + portlandite liquidus spans only a small temperature interval, 926–848 K (Gittins and Tuttle, 1964). Taking compositions at the end points and one intermediate point yields a regressed free energy equation of

$$\Delta\overline{G}_r^0 = 79.2\ (\pm 3.1) - 0.038\ (\pm 0.003)T\ \text{(kJ/mol)} \quad (25)$$

with $r^2 = 0.995$, where the uncertainties are only the 2σ standard errors of regression. This calibration is probably more uncertain than the regression errors would indicate, as potential experimental errors have not been included, and the temperature range of calibration is small.

However, the positive free energy for Reaction 21 implies that H_2O is preferentially partitioned into the vapor phase and that a H_2O-rich vapor would coexist with a relatively H_2O-poor carbonatite magma. If the regular solution model here is accurate, this calibration should be valid for all Ca-rich carbonate-rich melts, whether in synthetic or complex natural systems.

An example from nature. Within the Oka carbonatite complex, Quebec, Canada, is the Husereau carbonatite dike. That unique dike contains such a restrictive mineral assemblage that Treiman and Essene (1984) were able to calculate the composition of its F-poor vapor phase and infer by difference that the vapor was mostly H_2O. Gittins (1989) and Gittins et al. (1990) criticized their conclusion, asserting a much more prominent role for F. One source of disagreement was the abundance of F in a carbonatite magma compared with its vapor (Treiman and

Essene, 1992; Gittins et al., 1992). Application of the regular-solution model for carbonate-rich magmas can resolve this issue.

To calculate the concentrations of fluoride and OH in the Husereau carbonatite magma, one can apply Reactions 16 and 21 using the calibration in Equations 20 and 25. Treiman and Essene (1984) inferred that the Husereau carbonatite magma equilibrated with calcite, apatite, oxides, and other phases at 913 K and 1 kbar of total pressure. The gas phase was calculated to contain 110 bars CO_2; by difference, H_2O was inferred to account for 882 bars of the total vapor.

To calculate the abundance of OH in the Husereau dike magma, one can use the calculated composition of the Husereau gas phase in Reaction 21. Applying the calibration of Equation 25 yields

$$\frac{a^2_{OH^-,melt}}{a_{CO_3^{2-},melt}} = 2.8 \times 10^{-3}. \quad (26)$$

If one assumes the magma contained no abundant ion species besides carbonate and hydroxide, the regular-solution activity model (Eq. 5, Table 4), allows Equation 26 to be satisfied by $X_{OH^-} \approx 0.07$ and $X_{CO_3^{2-}} \approx 0.93$. This ratio is consistent with the absence of portlandite or other hydroxides as magmatic phases (viz., Gittins and Tuttle, 1964) and affirms that carbonatite magmas were much poorer in H_2O than their equilibrium vapors (here 882 bars H_2O and 110 bars CO_2). There is no mineralogic evidence for this abundance of magmatic OH in the Husereau dike, and one may speculate that it was expelled during solidification as a H_2O-rich vapor phase. Some of this H_2O-rich vapor might have been consumed in the pervasive conversion of magmatic periclase in the dike to brucite (Treiman and Essene, 1984), but most of it must have left the dike completely.

Fugacities of F-bearing gas species were calculated assuming F-OH exchange equilibria between apatite in the dike rock and vapor. From the inferred f_{O_2} of the QFM buffer ($10^{-18.6}$ bars), Treiman and Essene calculated that the gas fugacity of F_2 was $10^{-43.9}$ bars. From the temperature, gas fugacities, and Equation 20, one can now calculate the ratio of specie activities in the Husereau carbonatite melt as

$$\frac{a^2_{F^-,melt}}{a_{CO_3^{2-},melt}} = 4.8 \times 10^{-9}. \quad (27)$$

If the activity of carbonate in the melt was approximately unity, the activity of fluoride was 7×10^{-5}. The anion fraction of fluoride in the melt can be calculated knowing the anion fraction of carbonate in the melt, 0.93, as calculated above. This value gives a fluoride activity of 6.7×10^{-5} (Eq. 27), a fluoride activity coefficient of 1.06 (Eq. 19b), and so a fluoride anion fraction of 6.3×10^{-5}. Clearly, this is not much fluoride in the melt, and it is consistent with the lack of F-bearing minerals other than apatite in the dike. If the thermochemical analysis so far is correct, the only way for the melt to have had more F is for it to have been present in complexes, like molecular HF, SiF_6^{2-}, etc. There is no evidence for or against the presence of such fluoride complexes in the Husereau dike.

Carbonate magma on the surface of Venus

Carbonate-rich magmas may not be unique to the Earth, but may be of broader planetary importance, possibly occurring on Mars (Longhi, 1991) and Venus. The temperature and pressure of the Venus surface could be conducive to carbonate volcanism (Sill, 1984), and Magellan radar images of long sinuous channels on the Venus surface (presumably H_2O-free) have given that idea new life (Baker et al., 1992; Komatsu et al., 1992; Kargel et al., 1993). The possibility of carbonate magmas on Venus must be considered in the context of its surface conditions: a global mean temperature of 740 K and a mean atmospheric pressure of 95 bars (Seiff, 1983); the atmosphere consists of 96.5% CO_2, 3.5% N_2, and ~150 ppm SO_2 (Fegley et al., 1992). The Venera and VEGA chemical analyses of the Venus surface are consistent with tholeiitic or alkaline basalt, with two analyses suggesting felsic or peralkaline compositions (Barsukov, 1992).

Melting of calcite + anhydrite. Near-surface rocks on Venus are inferred to contain both calcite ($CaCO_3$) and anhydrite ($CaSO_4$) as weathering products of igneous minerals (Fegley and Prinn, 1989; Fegley et al., 1992); alkali carbonates and sulfates are not predicted to be significant in the weathering assemblage. Might calcite + anhydrite be molten under Venus surface conditions, or might calcite + anhydrite melt be formed under reasonable geological conditions (e.g., volcanic or impact heating)? On Venus, is it also possible that carbonate-sulfate magmas might be generated by liquid immiscibility from volatile-rich basaltic magma (Kargel et al., 1993)? Answering these questions requires knowing the liquidus surface in the system $CaCO_3$-$CaSO_4$, which can be calculated using the regular solution model developed here.

Melting relations in the system $CaCO_3$-$CaSO_4$ can be modeled with the thermochemical parameters derived and compiled here and compared with the experimentally determined phase equilibria of Fuerstenau et al. (1981). To calculate the liquidus surface, one requires heats of melting, temperatures of melting, solution models for calcite and anhydrite, and a solution model for their melts. Melting data for calcite are calculated for 100 bars from data in Tables 1 and 2. The melt solution of CO_3^{2-} and SO_4^{2-} is essentially ideal (Table 4). It is assumed that calcite and anhydrite are pure phases, that the $\Delta\overline{H}^0_{fus}$(anhydrite) is 28 kJ/mol, for a 1-bar melting temperature of 1723 K (Robie et al., 1979), and that this $\Delta\overline{H}^0_{fus}$(anhydrite) is relevant to 100 bars pressure. At 1468 K, anhydrite inverts to a high-temperature phase, which melts at 1737 ± 4 K (Rowe et al., 1965). The lower temperature chosen for this calculation is estimated for metastable melting of the lower temperature anhydrite polymorph, which would be stable at the Venus surface.

From these data and Equation 7, one can map the liquidus surface in $CaCO_3$-$CaSO_4$, ignoring the polymorphic transition in solid $CaSO_4$ (Fig. 3). The calcite-saturated and anhydrite-saturated liquidus curves are calculated independently. The intersection of the curves (the stable coexistence of calcite, anhydrite, and melt) at 1250 K is the eutectic point, the lowest temperature at which melt can exist in $CaCO_3$-$CaSO_4$. The eutectic temperature is 335 K below the melting temperature of calcite alone and 473 K below the melting temperature of anhydrite alone.

Predicted melting relations in $CaCO_3$-$CaSO_4$ are in partial accord with the experimental results of Fuerstenau et al. (1981), as shown in Figure 3. Fuerstenau et al. inferred phase relations by differential thermal analysis on sealed charges. They had little control on pressure, which was inferred to vary between 15 and 35 bars. Fuerstenau et al. did not analyze their experiment products, and so their identification of solid phases is completely by inference.

For the $CaCO_3$-rich calcite-saturated limb of the liquidus (Fig. 3), there is excellent agreement between the predictions here and the experiments of Fuerstenau et al. (1981). However, prediction and experiment do not agree for the $CaSO_4$-saturated limb of the liquidus. The experimental determination of this limb, inferred to be anhydrite + liquid (Fuerstenau et al., 1981), is not consistent with T_{fus}(anhydrite) = 1723 K (viz., Robie et al., 1979) but rather with $T_{fus} \approx 1550$ K (Fig. 3). Using the latter T_{fus} implies (by means of Eq. 6) that the $CaSO_4$-rich solid has $\Delta\overline{H}_{fus}$ per cation of ~28 kJ/mol, which is reasonable for an ionic compound. The source of these discrepancies is unclear; experimental error is possible, but a polymorphic transition in solid $CaSO_4$ is unlikely (Rowe et al., 1965). To me, it seems likely that the liquidus phase detected by Fuerstenau et al. (1981) is a previously unreported intermediate mixed-anion compound, for instance $Ca_3(SO_4)_2(CO_3)$, that melts incongruently to anhydrite + liquid.

Applying either predicted or experimental liquidus surfaces to Venus, one can see that mixtures of calcite + anhydrite will not melt at normal Venus surface temperatures, 660–760 K (Seiff, 1983). To melt a mixture of calcite + anhydrite on the Venus surface would require temperatures at least 500 K above ambient, which could easily be supplied by impact heating or basaltic volcanism (solidus temperatures near 1300–1400 K). Additional components, like alkalis or halides, would decrease the melting temperature, but the availability of these components is not clear. Similarly, the eutectic temperature calculated here does not invalidate the speculation that carbonate-sulfate magma could exsolve from basaltic magmas (Kargel et al., 1993).

F in Venus carbonatites. The near-surface atmosphere of Venus contains approximately 5 ppb of HF (Fegley et al., 1992), and one may inquire whether this much F in the atmosphere would significantly affect the compositions of ionic melts on the Venus surface. The model for fluorine-carbonate exchange between carbonate melts and vapor in Reaction 16 can be applied here, assuming that its free energy calibration (Eq. 20) can be extrapolated to 740 K from its minimum calibration temperature of 848 K. With thermochemical data from Robie et al. (1979) and the near-surface Venus atmospheric abundances of CO = ~20 ppm and H_2O = 20 ppm, the reactions

$$2HF + CO_2 \rightleftharpoons F_2 + H_2O + CO \qquad (28a)$$

and

$$2CO_2 \rightleftharpoons 2CO + O_2 \qquad (28b)$$

imply that $f_{F_2} = 1.1 \times 10^{-47}$ bars and $f_{O_2} = 3.5 \times 10^{-22}$ bars, within the magnetite stability field in Fe-O (Fegley et al., 1992). From Reaction 16 and its calibrations in Equations 17 and 20, one can now calculate the activity of fluoride in a carbonate-rich melt in equilibrium with the Venus atmosphere. With the derivation of Equation 21, fluoride and carbonate activities are related as

$$\frac{a^2_{F^-,melt}}{a_{CO_3^{2-},melt}} = 4.4 \times 10^{-5}. \qquad (29)$$

This implies that fluoride activity in a carbonate melt is, at most, 7×10^{-3}. The fluoride activity coefficient is unity in the absence of OH (Eq. 19b), implying the same value for the anion concentration of fluoride; this abundance corresponds to a F abundance of approximately 0.1 wt% (calculated for a melt containing only Ca^{2+}, CO_3^{2-}, and F^-). Thus, F from the atmosphere would be strongly concentrated in carbonate-rich melts on the Venus surface. However, the proportion of F would be so low as to have little effect in stabilizing those melts (Jago and Gittins, 1991).

Caveats

Caution must be exercised in applying this regular solution model of carbonate magmas, particularly in the precision of its implications. Many parameters in the model are poorly known, including heats of melting for magnesium carbonate and W interaction parameters for all cations with Mg^{2+}. The Temkin regular-solution model is only a first approximation to real behavior (Andersen and Kleppa, 1976) and can undoubtedly be improved given additional high-quality data. Finally, there remain the possibilities of multiple melt structures in Ca-rich carbonate magmas and of previously unreported liquidus phases in unexplored systems. It is hoped that this model can serve as a starting point for a deeper understanding of the thermochemical behavior of carbonate-rich magmas.

Acknowledgments

This work was started ten years ago during my doctoral studies at the University of Michigan, under the tutelage of E.J. Essene and W. Kelly, and with the assistance of L.M. Anovitz and J.W. Valley. More recently, I am grateful to B. Jago and J. Gittins for reviving my interest in carbonatite thermochemistry and to B. Fegley, Jr. and J. Kargel for collaborations on carbonate-sulfate magmas on Venus. The calculations here would have been impossible without the careful experiments reported over many years by P.J. Wyllie, J. Gittins, and their colleagues. This paper has ben-

efited from careful and constructive critiques by E.J. Essene, C.T. Herzberg, J.H. Jones, G. Ryder, B. Schuraytz, B.J. Wood, and an anonymous reviewer. Lunar and Planetary Institute contribution no. 840.

REFERENCES CITED

Andersen, B.K., and Kleppa, O.J. (1976) Enthalpies of mixing in binary liquid alkali carbonate solutions. Acta Chemica Scandinavica, A30, 751–758.

Andersen, D.J., and Lindsley, D.H. (1981) A valid Margules formulation for an asymmetric ternary solution: Revision of the olivine-ilmenite thermometer, with applications. Geochimica et Cosmochimica Acta, 45, 847–853.

Andersen, T. (1986) Magmatic fluids in the Fen carbonatite complex, S.E. Norway: Evidence of mid-crustal fractionation from solid and fluid inclusions in apatite. Contributions to Mineralogy and Petrology, 93, 491–503.

Anovitz, L.M., and Essene, E.J. (1987) Phase equilibria in the system $CaCO_3$-$MgCO_3$-$FeCO_3$. Journal of Petrology, 28, 389–414.

Bailey, D.K. (1993) Carbonate magmas. Journal of the Geological Society of London, 150, 637–651.

Baker, E.H. (1962) Calcium oxide-carbon dioxide system in the pressure range 1–300 atmospheres. Chemical Society Journal, 1962, 464–470.

Baker, R.V., Komatsu, G., Parker, T.J., Gulick, V.C., Kargel, J.S., and Lewis, J.S. (1992) Channels and valleys on Venus: Preliminary analysis of Magellan data. Journal of Geophysical Research, 97, 13421–13444.

Barsukov, V.L. (1992) Venusian igneous rocks. In V.L. Barsukov, A.T. Basilevsky, V.P. Volkov, and V.N. Zharkov, Eds., Venus geology, geochemistry, and geophysics, p. 165–176. University of Arizona Press, Tucson.

Berman, R.G., and Brown, T.H. (1987) Development of models for multicomponent melts: Analysis of synthetic systems. In Mineralogical Society of America Reviews in Mineralogy, 17, 405–442.

Biggar, G.M. (1969) Phase relationships in the join $Ca(OH)_2$-$CaCO_3$-$Ca_3(PO_4)_2$-H_2O at 1000 bars. Mineralogical Magazine, 37, 75–82.

Blander, M. (1964) Thermodynamic properties of molten salt solutions. In M. Blander, Ed., Molten salt chemistry, p. 127–237. Interscience, New York.

Blander, M., and Topol, L.E. (1966) The topology of phase diagrams of reciprocal molten salt systems. Inorganic Chemistry, 5, 1641–1645.

Bradley, R.S. (1962) Thermodynamic calculations on phase equilibria involving fused salts: I. General theory and application to equlibria involving calcium carbonate at high pressure. American Journal of Science, 260, 374–382.

Byrnes, A.P., and Wyllie, P.J. (1981) Subsolidus and melting relations for the join $CaCO_3$-$MgCO_3$ at 10 kbar. Geochimica et Cosmochimica Acta, 45, 321–328.

Carlson, W.D. (1983) The polymorphs of $CaCO_3$ and the aragonite-calcite transformation. In Mineralogical Society of America Reviews in Mineralogy, 11, 191–225.

Chase, M.W., Curnutt, J.L., Hu, A.T., Prophet, H., Syverud, A.N., and Walker, L.C. (1974) JANAF thermochemical tables: 1974 Supplement. Journal of Physical and Chemical Reference Data, 3, 311–480.

Cooper, A.F., Gittins, J., and Tuttle, O.F. (1975) The system Na_2CO_3-K_2CO_3-$CaCO_3$ at 1 kilobar and its significance in carbonatite petrogenesis. American Journal of Science, 275, 534–560.

Dawson, J.B., Garson, M.S., and Roberts, B. (1987) Altered former alkalic carbonatite lavas from Oldoinyo Lengai, Tanzania: Inferences for calcite carbonatite lavas. Geology, 15, 756–768.

Dawson, J.B., Pinkerton, H., Norton, G.E., and Pyle, D.M. (1990) Physicochemical properties of alkali carbonatite lavas: Data from the 1988 eruption of Oldoinyo Lengai, Tanzania. Geology, 18, 260–263.

DeKock, C.W. (1986) Thermodynamic properties of selected metal sulfates and their hydrates. Information Circular 9081: U.S. Bureau of Mines, 59 p. U.S. Government Printing Office, Washington, DC.

Eriksson, S.C. (1989) Phaloborwa: A saga of magmatism, metasomatism, and miscibility. In K. Bell, Ed., Carbonatites: Genesis and evolution, p. 221–254. Unwin-Hyman, Boston.

Fegley, B., Jr., and Prinn, R.G. (1989) Estimation of the rate of volcanism on Venus from reaction rate measurements. Nature, 337, 55–58.

Fegley, B., Jr., Treiman, A.H., and Sharpton, V.L. (1992) Venus surface mineralogy: Observations and theoretical constraints. Proceedings of Lunar and Planetary Science, 22, 3–20.

Fine, G., and Stolper, E. (1985) The speciation of carbon dioxide in sodium aluminosilicate glasses. Contributions to Mineralogy and Petrology, 91, 105–121.

Flood, H., Førland, T., and Roald, B. (1949) The equilibrium $CaCO_{3(melt)} = CaCO_{(s)} + CO_2$. The activity coefficients of calcium carbonate. Journal of the American Chemical Society, 71, 572–575.

Flood, H., Førland, T., and Motzfeld, K. (1952) On the oxygen electrode in molten salts. Acta Chemica Scandinavica, 6, 257–269.

Førland, T. (1955) An investigation of the activity of calcium carbonate in mixtures of fused salts. Journal of Physical Chemistry, 59, 152–156.

Fuerstenau, M.C., Shen, C.M., and Palmer, B.R. (1981) Liquidus temperatures in the $CaCO_3$-$Ca(OH)_2$-CaO and $CaCO_3$-$CaSO_4$-CaS ternary systems: II. Industrial and Engineering Chemical Process Design and Development, 20, 443–445.

Ghiorso, M.S. (1987) Modeling magmatic systems: Thermodynamic relations. In Mineralogical Society of America Reviews in Mineralogy, 17, 443–465.

Ghiorso, M.S., Carmichael, I.S.E., Rivers, M.L., and Sack, R.O. (1983) The Gibbs free energy of mixing in natural silicate liquids: An expanded regular solution approximation for the calculation of magmatic intensive variables. Contributions to Mineralogy and Petrology, 84, 107–145.

Gittins, J. (1989) The origin and evolution of carbonatite magmas. In K. Bell, Ed., Carbonatites: Genesis and evolution, p. 580–600. Unwin-Hyman, London.

Gittins, J., and Tuttle, O.F. (1964) The system CaF_2-$Ca(OH)_2$-$CaCO_3$. American Journal of Science, 262, 66–75.

Gittins, J., Beckett, M.F., and Jago, B.C. (1990) Composition of the fluid phase accompanying carbonatite magma: A critical examination. American Mineralogist, 75, 1106–1109.

——— (1992) Composition of the fluid phase accompanying carbonatite magma: A critical examination—Reply. American Mineralogist, 77, 666–667.

Helffrich, G., and Wood, B. (1989) Subregular model for multicomponent systems. American Mineralogist, 74, 1016–1022.

Helz, G.R., and Wyllie, P.J. (1979) Liquidus relationships in the system $CaCO_3$-$Ca(OH)_2$-CaS and the solubility of sulfur in carbonatite magmas. Geochimica et Cosmochimica Acta, 43, 259–265.

Hogarth, D.D. (1989) Pyrochlore, apatite, and amphibole: Distinctive minerals in carbonatite. In K. Bell, Ed., Carbonatites: Genesis and evolution, p. 105–148. Unwin-Hyman, London.

Huang, W.-L., and Wyllie, P.J. (1976) Melting relationships in the system CaO-CO_2 and MgO-CO_2 to 33 kilobars. Geochimica et Cosmochimica Acta, 40, 129–132.

Irving, A.J., and Wyllie, P.J. (1973) Melting relationships in CaO-CO_2 and MgO-CO_2 to 36 kilobars with comments on CO_2 in the mantle. Earth and Planetary Science Letters, 20, 220–225.

——— (1975) Solidus and melting relationships for calcite, magnesite, and the join $CaCO_3$-$MgCO_3$ to 36 kilobars. Geochimica et Cosmochimica Acta, 39, 35–53.

Jago, B.C., and Gittins, J. (1991) The role of fluorine in carbonatite magma evolution. Nature, 349, 56–58.

Janz, G.J., Allen, D.B., Bansal, N.P., Murphy, R.M., and Tompkins, R.P.T. (1979) Physical properties data compilations relevant to energy storage: II. Molten salts: Data on single and multi-component systems. National Standards Reference Data Series. NSRDS-NBS 61, Part II. U.S. Government Printing Office, Washington, DC.

Jones, A.P., and Wyllie, P.J. (1986) Solubility of rare earth elements in carbonatite magmas, indicated by the liquidus surface in $CaCO_3$-$Ca(OH)_2$-$La(OH)_3$. Applied Geochemistry, 1, 95–102.

Kargel, J.S., Komatsu, G., Baker, R.V., and Strom, R.G. (1993) The volcanology of Venera and VEGA landing sites and the geochemistry of Venus. Icarus, 103, 253–275.

Keller, J., and Krafft, M. (1990) Effusive natrocarbonatite activity of Oldoinyo Lengai, June 1988. Bulletin of Volcanology, 52, 629–645.

Kjarsgaard, B.A., and Hamilton, D.J. (1989) The genesis of carbonatites by immiscibility. In K. Bell, Ed., Carbonatites: Genesis and evolution, p. 388–404. Unwin-Hyman, London.

Klement, W., Jr., and Cohen, L.H. (1975) Solid-solid and solid-liquid

transitions in K_2CO_3, Na_2CO_3, and Li_2CO_3: Investigations to >5 kbar by differential thermal analysis; thermodynamics and structural correlations. Berichte der Bunsengesellschaft, 79, 327–334.

Kleppa, O.J. (1977) Thermodynamic properties of molten salt solutions. In D.G. Fraser, Ed., Thermodynamics in geology, p. 279–299. Reidel, Boston.

——— (1981) Thermodynamics of simple molten salt mixtures. In R.C. Newton, A. Navrotsky, and B.J. Wood, Eds., Thermodynamics of minerals and melts, p. 179–188. Springer, New York.

Kleppa, O.J., and Julsrud, S. (1980) Thermodynamics of charge-unsymmetrical anion mixtures: I. The liquid systems AF-A_2SO_4. Acta Chemica Scandinavica, A34, 655–665.

Komatsu, G., Kargel, J.S., and Baker, V.R. (1992) Canali-type channels on Venus: Some genetic constraints. Geophysics Research Letters, 19, 11415–11418.

Koster van Groos, A.F., and Wyllie, P.J. (1966) Liquid immiscibility in the system Na_2O-Al_2O_3-SiO_2-CO_2 at pressures to 1 kilobar. American Journal of Science, 264, 234–255.

Kresten, P., and Morogan, V. (1986) Fenitization at the Fen complex, southern Norway. Lithos, 19, 27–42.

Kuellmer, F.J., Visocky, A.P., and Tuttle, O.F. (1966) Preliminary survey of the system barite-calcite-fluorite at 500 bars. In O.F. Tuttle and J. Gittins, Eds., Carbonatites, p. 353–364. Wiley, London.

Lapin, A.V. (1976) Geological examples of limited miscibility in ore-silicate-carbonate melts. Døklady Akademie Nauk SSSR, 231, 163–166.

LeBas, M.J. (1977) Carbonatite-nephelinite volcanism, 347 p. Wiley, New York.

——— (1981) Carbonatite magmas. Mineralogical Magazine, 44, 133–140.

Levin, E.M., Robbins, C.R., and McMurdie, H.F. (1964) Phase diagrams for ceramists, vol. 1, 601 p. American Ceramic Society, Columbus, Ohio.

——— (1969) Phase diagrams for ceramists, vol. 2, 625 p. American Ceramic Society, Columbus, Ohio.

Lewis, G.N., and Randall, M. (1961) Thermodynamics (2nd edition), (revised by Pitzer, K.J., and Brewer, L.), 723 p. McGraw-Hill, New York.

Longhi, J. (1991) Complex magmatic processes on Mars: Inferences from the SNC meteorites. Proceedings of Lunar and Planetary Science, 21, 695–709.

Lumsden, J. (1966) Thermodynamics of molten salt mixtures, 146 p. Academic Press, New York.

McKie, D. (1966) Fenitization. In O.F. Tuttle and J. Gittins, Eds., Carbonatites, p. 261–294. Wiley, London.

McSwiggen, P.L. (1993) Alternative solution model for the ternary carbonate system $CaCO_3$-$MgCO_3$-$FeCO_3$: II. Calibration of a combined ordering model and mixing model. Physics and Chemistry of Minerals, 20, 42–55.

Mirwald, P.W. (1979) Determination of a high-temperature transition of calcite at 800°C and 1 bar CO_2 pressure. Neues Jahrbuch für Mineralogie Monatshefte, 309–315.

Mysen, B.O., and Virgo, D. (1980) Solubility mechanisms of carbon dioxide in silicate melts: A Raman spectroscopic study. American Mineralogist, 65, 885–899.

Nesbitt, B.E., and Kelly, W.C. (1977) Magmatic and hydrothermal inclusions in carbonatites of the Magnet Cove complex, Arkansas. Contributions to Mineralogy and Petrology, 63, 271–294.

Norton, G.E., and Pinkerton, H. (1992) The physical properties of carbonatite lavas: Implications for planetary volcanism (abs.). Lunar and Planetary Science, 23, 1001–1002.

Peterson, T.D. (1990) Petrology and genesis of natrocarbonatite. Contributions to Mineralogy and Petrology, 105, 143–155.

Poletaev, I.F., Lyudomirskaya, A.P., and Tsiklina, N.D. (1975) Equilibrium diagram of the system $CaCO_3$ + Na_2SO_4 ⇌ $CaSO_4$ + Na_2CO_3. Russian Journal of Inorganic Chemistry, 20, 1742–1743.

Ragone, S.E., Datta, R.K., Roy, D.M., and Tuttle, O.F. (1966) The system potassium carbonate-magnesium carbonate. Journal of Chemical Physics, 70, 2260–2261.

Rankin, A.H. (1975) Fluid inclusion studies in apatites from carbonatites of the Wasaki area of western Kenya. Lithos, 8, 123–136.

Robie, R.A., Hemingway, B.S., and Fisher, J.R. (1979) Thermodynamic properties of minerals and related substances at 298.15 K and 1 bar (10^5 pascals) pressure and at higher temperatures, corrected, 456 p. U.S. Geological Survey Bulletin 1452. U.S. Government Printing Office, Washington, DC.

Rowe, J.J., Morey, G.W., and Hansen, I.D. (1965) The binary system K_2SO_4-$CaSO_4$. Journal of Inorganic and Nuclear Chemistry, 27, 53–58.

Rubie, D.C., and Gunter, W.D. (1983) The role of speciation in alkaline igneous fluids during fenite metasomatism. Contributions to Mineralogy and Petrology, 82, 165–175.

Seiff, A. (1983) Thermal structure of the atmosphere of Venus. In D.M. Hunten et al., Eds., Venus, p. 215–279. University of Arizona Press, Tucson.

Selman, J.R., and Maru, H.C. (1981) Physical chemistry and electrochemistry of alkali carbonate melts, with special reference to molten-carbonate fuel cells. In G. Mamantov and J. Braunstein, Eds., Advances in molten salt chemistry, vol. 4, p. 159–389. Plenum, New York.

Sill, G.T. (1984) Possible carbonatite volcanism on Venus (abs.). Bulletin of the American Astronomical Society, 16, 696.

Sundheim, B.R., Ed. (1964) Fused salts, 435 p. McGraw-Hill, New York.

Tacker, R.C., and Stormer, J.C. (1993) Thermodynamics of mixing of liquids in the system $Ca_3(PO_4)_2$-$CaCl_2$-CaF_2-$Ca(OH)_2$. Geochimica et Cosmochimica Acta, 57, 4663–4676.

Temkin, M. (1945) Mixtures of fused salts as ionic solutions. Acta Physicochimica USSR, 20, 411–420.

Treiman, A.H. (1989) Carbonatite magma: Properties and processes. In K. Bell, Ed., Carbonatites: Genesis and evolution, p. 89–104. Unwin-Hyman, London.

Treiman, A.H., and Essene, E.J. (1984) A periclase-dolomite-calcite carbonatite from the Oka complex, Quebec, and its calculated volatile composition. Contributions to Mineralogy and Petrology, 85, 149–157.

Treiman, A.H., and Essene, E.J. (1985) The Oka carbonatite complex, Quebec: Geology and evidence for silicate-carbonate liquid immiscibility. American Mineralogist, 70, 1101–1113.

Treiman, A.H., and Essene, E.J. (1992) Composition of the fluid phase accompanying carbonatite magmas: A critical examination—Discussion. American Mineralogist, 77, 663–665.

Treiman, A.H., and Schedl, A. (1983) Properties of carbonatite magma and processes in carbonatite magma chambers. Journal of Geology, 91, 437–447.

Watson, E.B. (1991) Diffusion in fluid-bearing and slightly-melted rocks: Experimental and numerical approaches illustrated by iron transport in dunite. Contributions to Mineralogy and Petrology, 107, 417–434.

Wyllie, P.J. (1989) Origin of carbonatites: Evidence from phase equilibrium studies. In K. Bell, Ed., Carbonatites: Genesis and evolution, p. 500–545. Unwin-Hyman, London.

Wyllie, P.J., and Haas, J.L. (1965) The system CaO-SiO_2-CO_2-H_2O: I. Melting relationships with excess vapor at 1 kilobar pressure. Geochimica et Cosmochimica Acta, 29, 871–892.

Wyllie, P.J., and Tuttle, O.F. (1960) The system CaO-CO_2-H_2O and the origin of carbonatites. Journal of Petrology, 1, 1–46.

Zarzycki, J. (1962) High-temperature X-ray diffraction studies of fused salts: Structures of molten alkali carbonates and sulfates. Discussions of the Faraday Society, 32, 38–48.

Manuscript received December 30, 1993
Manuscript accepted July 27, 1994